SCIENCE CHINA
Chemistry

• ARTICLES •

July 2016 Vol.59 No.7: 878–894
doi: 10.1007/s11426-015-0351-0

Coumarin-derived azolyl ethanols: synthesis, antimicrobial evaluation and preliminary action mechanism

Xin-Mei Peng, Kannekanti Vijaya Kumar†, Guri L.V. Damu† & Cheng-He Zhou*

Institute of Bioorganic & Medicinal Chemistry; Key Laboratory of Applied Chemistry of Chongqing Municipality; School of Chemistry and Chemical Engineering, Southwest University, Chongqing 400715, China

Received August 23, 2015; accepted September 7, 2015; published online May 31, 2016

A series of coumarin-derived azolyl ethanols including imidazolyl, triazolyl, tetrazolyl, benzotriazolyl, thiol-imidazolyl and thiol-triazolyl ones were conveniently synthesized and characterized by IR, ^{1}H NMR, ^{13}C NMR and high-resolution mass spectra (HRMS) spectra. Some of the prepared compounds showed appropriate logP_{ow} values and effective antibacterial and antifungal activities. Noticeably, compound **14** with bis-triazolyl ethanol group exhibited low minimal inhibitory concentration (MIC) value of 8 μg/mL against MRSA, which was comparable or even superior to reference drugs Norfloxacin (MIC=8 μg/mL) and Chloramphenicol (MIC=16 μg/mL). It could also effectively inhibit the growth of the tested fungal strains compared to Fluconazole. Further binding studies of coumarin **14** with calf thymus DNA were investigated by UV-Vis absorption and fluorescence spectroscopy. It was found that compound **14** could interact with calf thymus DNA by groove binding to form **14**-DNA complex via both hydrogen bonds and van der Waals force, which might be the factor to exert the powerful antimicrobial activity.

coumarin, imidazole, triazole, tetrazole, antibacterial, antifungal, calf thymus DNA

Citation: Peng XM, Kumar KV, Damu GLV, Zhou CH. Coumarin-derived azolyl ethanols: synthesis, antimicrobial evaluation and preliminary action mechanism. *Sci China Chem*, 2016, 59: 878–894, doi: 10.1007/s11426-015-0351-0

1 Introduction

Bacterial and fungal infections have been remaining quite prevalent in recent years. Various antibiotics including beta-lactams, tetracyclines, aminoglycosides, macrolides, polyenes *etc.* and artificial synthetic drugs such as sulfonamides, quinolones, oxazolidones, azoles, allylamines and so on are available throughout the world, however, the indiscriminate use of antiinfective drugs for the prevention and treatment of diseases has accelerated the emergence of drug-resistant strains [1]. Especially methicillin-resistant *Staphylococcus aureus* (MRSA), methicillin-resistant *Staphylococcus epidermidis* (MRSE), vancomycin-resistant *Enterococccus faecium* (VRE) and carbapenems-resistant *Enterobacteriaceae* (e.g. NDM-1) make a great deal of traditional antibiotics decrease their effects or totally lose activities [2,3]. On the other hand, the mortality and morbidity of opportunistic fungal infections are exponentially increasing and the number of fatal incidence resulted from fungi is becoming comparable with that of tuberculosis and malaria due to the increasing number of patients with organ and stem cell transplantation, with HIV/AIDS and with other immune compromised diseases [4]. This situation stimulates an urgent need to develop more effective antimicrobial

*Corresponding author (email: zhouch@swu.edu.cn)
†Postdoctoral fellow from Indian Institute of Chemical Technology, Hyderabad 500607, India

agents.

Metronidazole (**I**), Secnidazole (**II**) and Ornidazole (**III**) are well-known clinical antibacterial drugs for their bactericidal and archaeacidal activity against anaerobicbacteria and methanogenic archaea [5,6]. Fluconazole (**IV**) and Voriconazole (**V**) are the most widely used antifungal agents in the treatment of invasive fungal infections because of safety profile, orally effective property and high therapeutic index [7,8]. From the structures of these drugs, it is obvious that the azolyl ethanol fragment plays an important role in exerting antimicrobial activity. Our previous work has introduced the azolyl ethanol moiety into quinolones to afford a series of hybrids, which exhibited strong efficiency against all the tested bacterial and fungal strains. Compound **VI** could not only effectively inhibit the growth of the tested fungi (minimal inhibitory concentration, MIC=0.5 μg/mL) compared to Fluconazole (MIC=0.5 μg/mL), but also display MIC values ranging from 0.25 to 1 μg/mL against all the tested bacteria, which was comparative or much superior to Clinafloxacin and Chloramphenicol [9]. Nitroimidazolyl ethanol (**VII**) showed a low MIC value of 0.39 nmol/L against MRSA compared to reference drugs Chloramphenicol and Norfloxacin [10]. While triazolyl ethanol modified quinolone **VIII** exhibited good antibacterial and antifungal activity against all the tested strains with MIC values between 0.5 and 32 μg/mL except for *Candida utilis* [11]. All the results clearly indicated that the introduction of azolyl ethanol moiety into quinolones could not only remarkably enhance the antimicrobial activities, but also overcome the drug-resistance and/or broaden the antimicrobial spectrum.

Literature has revealed that the introduction of sulfur atom into azolyl compounds is beneficial for bioactivities [12]. The presence of sulfur atom might be able to improve the lipophilicity and modulate electron density of target compounds, thereby influencing their transmembrane diffusion abilities and interactions with hydrogen bond donors in organisms [13]. In antimicrobial fields, the investigations of sulfur-containing azoles such as azole-thioethers have become increasingly attractive in recent years [14].

Coumarin derivatives have gained great therapeutic importance in the field of medicinal chemistry due to their extensively biological activities such as antibacterial, antifungal, antiviral, antitubercular, antimalarial, anticoagulant, antiinflammatory, anticancer, antioxidant properties [15]. Coumarins with benzopyrone skeleton are structurally similar to clinical antiinfective quinolones with benzopyridone backbone, which can inhibit ATPase activity of bacterial DNA gyrase by competing with ATP binding to the B subunit of the enzyme to exert antibacterial ability [16,17]. Especially, researches have revealed that coumarin compounds possess prominent antibacterial properties against MRSA and MRSE [18]. For this reason, the positive investigations towards coumarin compounds for potential antimicrobial agents are renewing upsurge (Figure 1).

In view of the above observations, considering the importance of azolyl ethanol fragment and coumarin compounds, and as an extension of our researches on bioactive heterocyclic compounds [19], herein we incorporated azolyl ethanol group into coumarin skeleton to generate a series of coumarin-derived azolyl ethanols as potential antimicrobial agents. The target compounds were designed based on the following considerations:

(1) Imidazolyl ethanol fragments, especially nitroimidazolyl ethanol one not only could enhance the antimicrobial activities of target compounds, but also was beneficial to form hydrogen bonds at resistance mutation region of resis-

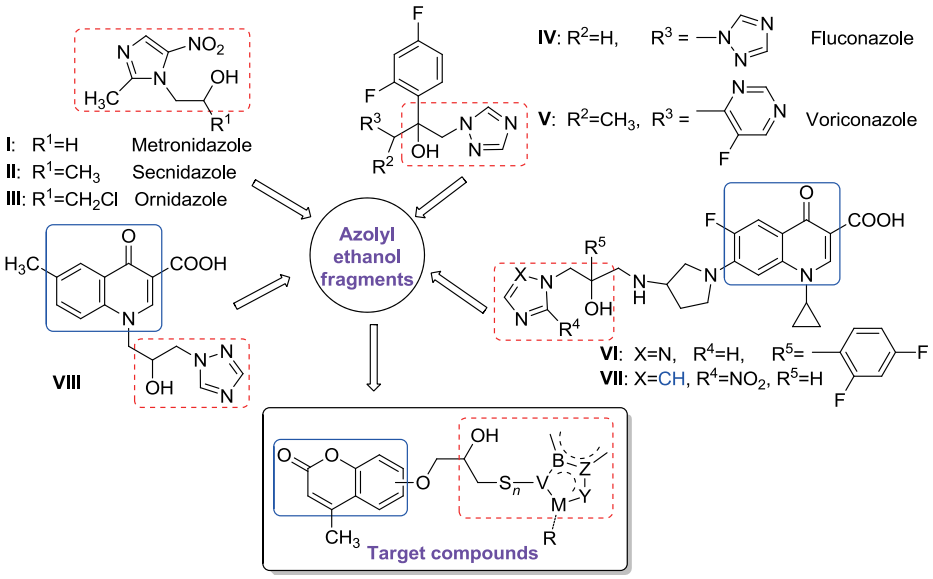

Figure 1 Design of coumarin-derived azolyl ethanols as antimicrobial agents.

tant bacteria such as MRSA [20]. Therefore, imidazolyl ethanol moiety was introduced into coumarin ring to afford compound **4**.

(2) It is well known that the triazolyl ethanol group in Fluconazole is vital in exerting excellent antifungal activity *in vivo* [21]. Other compounds containing triazolyl ethanol fragment were also found to be effective against bacterial and fungal strains [9,11]. In view of this, coumarin-derived triazolyl ethanol **5** was prepared.

(3) Tetrazolyl ethanol moiety and benzotriazolyl ethanol one could be viewed as isostere of imidazolyl and triazolyl ethanol fragments in designing drug molecules. Thereby, tetrazolyl and benzotriazolyl ethanol groups were studied to explore their effect on the physicochemical properties and antimicrobial efficacies of the designed compounds.

(4) Literature has confirmed that thioether-containing compounds could effectively increase biological activities and broaden antimicrobial spectrum and act a mechanism as ribosome-targeting activity [22]. To this end, coumarin-based thio-imidazolyl and thio-triazolyl ethanols were obtained.

(5) Our previous work has revealed that bis-triazolyl coumarin exhibited excellent antibacterial and antifungal ability [17]. In order to investigate the influence of the number of azolyl ethanol fragment on the bioactivities of target compounds, bis-azolyl ethanol fragment modified coumarins **13**−**17** were designed.

All the newly synthesized compounds were evaluated for their antibacterial and antifungal activities *in vitro* against three Gram-positive bacteria, three Gram-negative bacteria and five fungi.

The exploration of interactions between drugs or bioactive small molecules and DNA are beneficial to provide possible mechanism of agents, and to make further help for the design, modification and screening of new drug molecules. So we further investigated the preliminary binding mechanism of the most highly active compound with calf thymus DNA [23].

2 Experimental

2.1 Materials and measurements

Melting points were recorded on X-6 melting point apparatus and uncorrected. Thin layer chromatography (TLC) analysis was done using precoated silica gel plates. Fourier transform infrared spectroscopy (FTIR) spectra were carried out on Bruker RFS100/S spectrophotometer (Bio-Rad, USA) using KBr pellets in the 400–4000 cm^{-1} range. ^{1}H and ^{13}C NMR spectra were recorded on Bruker AV 300 spectrometer and AVANCE III 600 spectrometer (Bruker BioSpin AG Ltd., China) using TMS as an internal standard. The chemical shifts were reported in parts per million (ppm), the coupling constants (*J*) were expressed in hertz (Hz) and signals were described as singlet (s), doublet (d), triplet (t) as well as multiplet (m). The high-resolution mass spectra (HRMS) were recorded on IonSpec FT-ICR mass spectrometer with ESI resource. All the fluorescence spectra were recorded at 290, 300, 310 K in the range of 340–600 nm on F-7000 Spectrofluorimeter (Hitachi, Japan) equipped with 1.0 cm quartz cells, the widths of both the excitation and emission slit were set as 5 nm, and the excitation wavelength was 323 nm. UV spectra were recorded at room temperature on a TU-2450 spectrophotometer (Puxi Analytic Instrument Ltd. of Beijing, China) equipped with 1.0 cm quartz cells. Calf thymus DNA and NR were obtained from Sigma-Aldrich (St. Louis, USA). Tris(hydroxymethyl) aminomethane (Tris) and concentrated HCl were analytical purity. Sample masses were weighed on a microbalance with a resolution of 0.1 mg. All other chemicals and solvents were commercially available, and used without further purification.

2.2 Synthesis

The synthetic route of coumarin-derived azolyl ethanols was outlined in Schemes 1 and 2. The desired target compounds were synthesized via multistep reactions from commercially available phenols, ethyl acetoacetate and concentrated sulfuric acid. Intermediates **3** and **12** were prepared by the *O*-alkylation of 2-(chloromethyl)oxirane with hydroxyl coumarins **2** and **11** in yields of 91.3% and 80.1%, respectively. The reactions of compounds **3** and **12** via the opened ring by various azoles in ethanol using potassium carbonate as base afforded the corresponding mono-azolyl ethanols **4**−**9** and bis-azolyl ethanols **13**−**17**.

2.2.1 Compounds **2**, **3**, **11** and **12**

Compounds **2**, **3**, **11** and **12** were prepared according to the literature methods [17,24].

2.2.2 7-(2-Hydroxy-3-(1*H*-imidazol-1-yl)propoxy)-4-methyl-2*H*-chromen-2-one (**4a**)

To a stirred suspension of potassium carbonate (0.166 g, 1.2 mmol) in ethanol (8 mL) was added 1*H*-imidazole (0.068 g, 1 mmol). The mixture was stirred at 60 °C for 1 h and then cooled to room temperature. Compound **3** (0.232 g, 1 mmol) was added and stirred under 70 °C. After the reaction was completed (monitored by TLC, chloroform/methanol, 30:1, *V*/*V*), the solvent was evaporated and the residue was treated with water (15 mL) and extracted with chloroform (3×15 mL). The combined organic phase was dried over anhydrous sodium sulfate and concentrated under the reduced pressure. The crude product was purified by silica gel column chromatography (eluent, chloroform/methanol, 50:1–30:1, *V*/*V*) to afford the pure compound **4a** (0.142 g) as white solid. Yield: 47.2%; mp: 155–157 °C; IR (KBr) *v*: 3489 (OH), 3090, 3070 (aromatic C–H), 2983, 2856 (aliphatic C–H), 1725 (C=O), 1601, 1565, 1498 (aromatic frame), 1353, 1319, 1268, 1157, 1104, 1072, 1009, 982, 880, 823 cm^{-1}; ^{1}H NMR

(600 MHz, DMSO-d_6) δ: 7.69 (d, J=9.2 Hz, 1H, coumarin 5-*H*), 7.60 (s, 1H, imidazole 2-*H*), 7.17 (d, J=8.5 Hz, 1H, imidazole 4-*H*), 6.99 (d, J=6.7 Hz, 2H, coumarin 6,8-*H*), 6.88 (d, J=5.2 Hz, 1H, imidazole 5-*H*), 6.22 (s, 1H, coumarin 3-*H*), 5.56 (s, 1H, O*H*), 4.19–4.11 (m, 2H, coumarin-OCH_2), 4.07 (dd, J=13.4, 7.0 Hz, 1H, C*H*OH), 3.96–3.89 (m, 2H, imidazole-CH_2), 2.40 (s, 3H, coumarin 4-CH_3) ppm; ^{13}C NMR (150 MHz, DMSO-d_6) δ: 161.9, 160.5, 155.1, 153.8, 138.3, 128.5, 126.9, 120.5, 113.8, 112.9, 111.7, 101.8, 70.6, 68.5, 49.6, 18.5 ppm; HRMS (ESI) calcd. for $C_{16}H_{16}N_2O_4$ $[M+H]^+$, 301.1188, found, 301.1190, $[M+Na]^+$, 323.1008, found, 323.1006.

2.2.3 7-(2-Hydroxy-3-(2-phenyl-1*H*-imidazol-1-yl) propoxy)-4-methyl-2*H*-chromen-2-one (**4b**)

Compound **4b** (0.089 g) was obtained as white solid according to general procedure described for **4a** starting from potassium carbonate (0.166 g, 1.2 mmol), 2-phenyl-1*H*-imidazole (0.144 g, 1 mmol) and compound **3** (0.232 g, 1 mmol). Yield: 23.6%; mp: 115–117 °C; IR (KBr) *v*: 3447 (OH), 3097, 3065

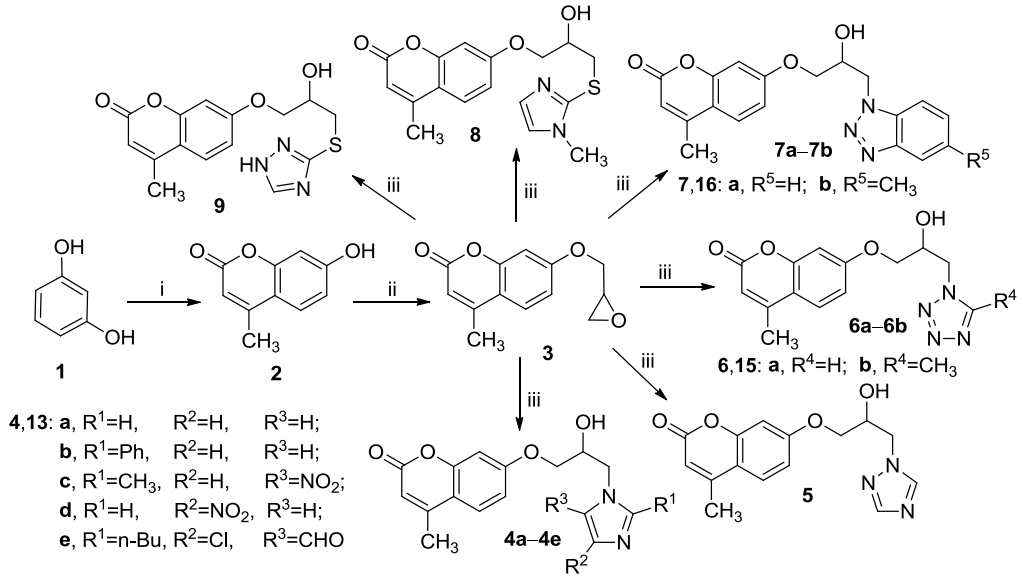

Scheme 1 Synthetic route of coumarin-derived mono-azolyl ethanols. Reagents and conditions: (i) ethyl acetoacetate, concentrated H_2SO_4, 0–5 °C, 2–3 h; (ii) epichlorohydrin, K_2CO_3, reflux, 4–6 h; (iii) azoles, K_2CO_3, EtOH, 70 °C, 2–4 h.

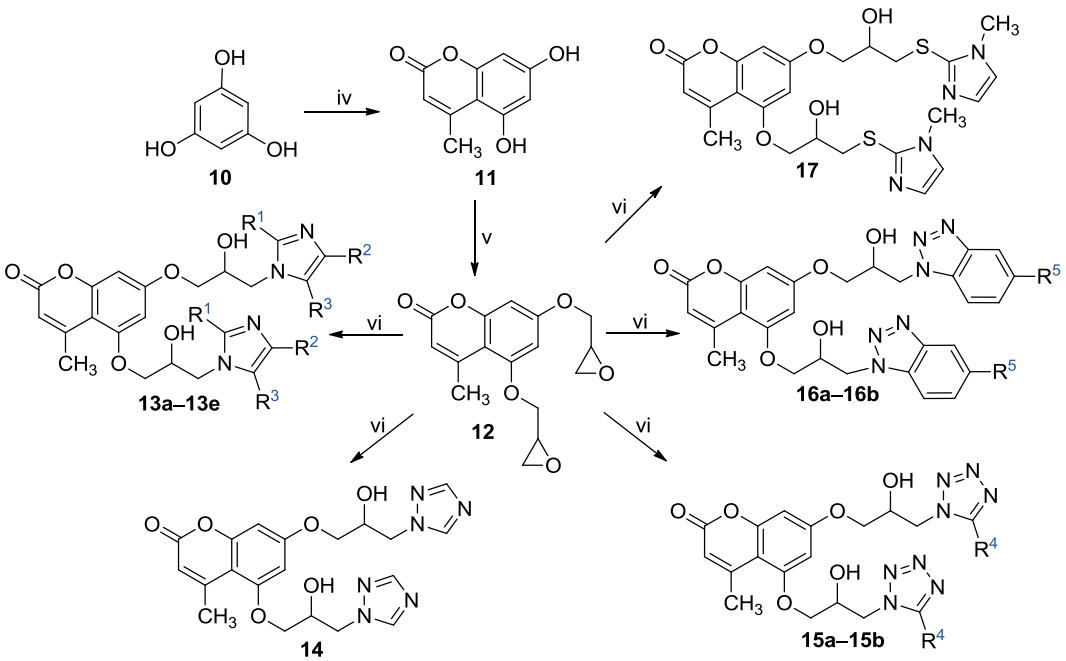

Scheme 2 Synthetic route of coumarin-derived bis-azolyl ethanols. Reagents and conditions: (iv) ethyl acetoacetate, concentrated H_2SO_4, 0–5 °C, 2–3 h; (v) epichlorohydrin, K_2CO_3, reflux, 4–6 h; (vi) azoles, K_2CO_3, EtOH, 70 °C, 2–4 h.

(aromatic C–H), 2986, 2845 (aliphatic C–H), 1724 (C=O), 1596, 1546, 1506, 1489 (aromatic frame), 1291, 1266, 1167, 1096, 1072, 950, 898, 867 cm^{-1}; ^1H NMR (600 MHz, DMSO-d_6) δ: 7.69–7.64 (m, 3H, coumarin 5-*H*, phenyl 2,6-*H*), 7.48–7.42 (m, 3H, phenyl 3,4,5-*H*), 7.40 (d, *J*=8.5 Hz, 1H, idaimzole 4-*H*), 7.06 (d, *J*=8.5 Hz, 1H, imidazole 5-*H*), 6.90–6.82 (m, 2H, coumarin 6,8-*H*), 6.22 (s, 1H, coumarin 3-*H*), 5.63 (s, 1H, O*H*), 4.27–4.11 (m, 3H, coumarin-OCH_2, C*H*OH), 3.99–3.93 (m, 2H, imidazole-CH_2), 2.40 (s, 3H, coumarin 4-CH_3) ppm; ^{13}C NMR (150 MHz, DMSO-d_6) δ: 162.7, 160.1, 158.7, 156.8, 154.3, 152.8, 144.9, 129.6, 127.6, 124.5, 123.2, 122.2, 113.7, 105.7, 96.8, 94.2, 71.5, 68.5, 49.1, 24.5 ppm; HRMS (ESI) calcd. for $C_{22}H_{20}N_2O_4$ $[M+H]^+$, 377.1501, found, 377.1504.

2.2.4 7-(2-Hydroxy-3-(2-methyl-5-nitro-1*H*-imidazol-1-yl) propoxy)- 4-methyl-2*H*-chromen-2-one(**4c**)

Compound **4c** (0.221 g) was obtained as yellow solid according to general procedure described for **4a** starting from potassium carbonate (0.166 g, 1.2 mmol), 2-methyl-5-nitro-1*H*-imidazole (0.127 g, 1 mmol) and compound **3** (0.232 g, 1 mmol). Yield: 61.4%; mp: 174–176 °C; IR (KBr) *v*: 3426 (OH), 3126, 3065 (aromatic C–H), 2956, 2814 (aliphatic C–H), 1714 (C=O), 1597, 1544, 1506, 1467 (aromatic frame), 1391, 1266, 1203, 1072, 1042, 997, 950, 844, 814 cm^{-1}; ^1H NMR (300 MHz, DMSO-d_6) δ: 8.29 (s, 1H, imidazole 4-*H*), 7.73 (d, 1H, *J*=9 Hz, coumarin 5-*H*), 7.04 (d, 1H, *J*=6 Hz, coumarin 6-*H*), 6.99 (s, 1H, coumarin 8-*H*), 6.24 (s, 1H, coumarin 3-*H*), 5.69 (d, 1H, *J*=6 Hz, O*H*), 4.26–4.22 (m, 2H, phenyl-OCH_2), 4.11–4.09 (m, 3H, C*H*OHCH_2), 2.41 (s, 3H, imidazole 2-CH_3), 2.38 (s, 3H, coumarin 4-CH_3) ppm; ^{13}C NMR (75 MHz, DMSO-d_6) δ: 161.7, 160.5, 155.1, 153.8, 146.1, 145.7, 126.9, 123.2, 113.7, 112.9, 111.7, 101.7, 70.5, 68.1, 49.8, 18.5, 13.3 ppm; HRMS (ESI) calcd. for $C_{17}H_{17}N_3O_6$ $[M+H]^+$, 360.1196, found, 360.1198.

2.2.5 7-(2-Hydroxy-3-(4-nitro-1*H*-imidazol-1-yl) propoxy)-4-methyl-2*H*-chromen-2-one (**4d**)

Compound **4d** (0.209 g) was obtained as yellow solid according to general procedure described for **4a** starting from potassium carbonate (0.166 g, 1.2 mmol), 4-nitro-1*H*-imidazole (0.113 g, 1 mmol) and compound **3** (0.232 g, 1 mmol). Yield: 60.6%; mp: 186–188 °C; IR (KBr) *v*: 3428 (OH), 3136, 3075 (aromatic C–H), 2976, 2854 (aliphatic C–H), 1717 (C=O), 1607, 1574, 1546, 1497 (aromatic frame), 1374, 1316, 1276, 1159, 1092, 1031, 850, 834, 762 cm^{-1}; ^1H NMR (300 MHz, DMSO-d_6) δ: 8.23 (s, 1H, imidazole 5-*H*), 7.94 (s, 1H, imidazole 2-*H*), 7.79 (d, 1H, *J*=9 Hz, coumarin 5-*H*), 7.14 (d, 1H, *J*=6 Hz, coumarin 6-*H*), 6.97 (s, 1H, coumarin 8-*H*), 6.22 (s, 1H, coumarin 3-*H*), 5.67 (d, 1H, *J*=6 Hz, O*H*), 4.29–4.26 (m, 2H, phenyl-OCH_2), 4.12–4.06 (m, 3H, C*H*OHCH_2), 2.40 (s, 3H, coumarin 4-CH_3) ppm; ^{13}C NMR (75 MHz, DMSO-d_6) δ: 161.5, 160.7, 155.8, 153.1, 146.7, 145.1, 126.2, 123.7, 113.9, 112.4, 111.7, 101.9, 70.4, 68.1, 49.3, 18.3 ppm; HRMS (ESI) calcd. for $C_{16}H_{15}N_3O_6$ $[M+H]^+$, 346.1039, found, 346.1038.

2.2.6 2-Butyl-4-chloro-1-(2-hydroxy-3-(4-methyl-2-oxo-2*H*-chromen-7-yloxy)propyl)-1*H*-imidazole-5-carbaldehyde (**4e**)

Compound **4e** (0.117 g) was obtained as yellow solid according to general procedure described for **4a** starting from potassium carbonate (0.166 g, 1.2 mmol), 2-butyl-4-chloro-1*H*-imidazole-5-carbaldehyde (0.187 g, 1 mmol) and compound **3** (0.232 g, 1 mmol). Yield: 28.1%; mp: 71–73 °C; IR (KBr) *v*: 3408 (OH), 3096, 3025 (aromatic C–H), 2987, 2843 (aliphatic C–H), 1725 (C=O), 1602, 1589, 1556, 1507 (aromatic frame), 1324, 1296, 1155, 1123, 1086, 1035, 889, 867 cm^{-1}; ^1H NMR (600 MHz, DMSO-d_6) δ: 9.60 (s, 1H, C*H*O), 7.71 (d, *J*=8.7 Hz, 1H, coumarin 5-*H*), 6.99 (t, *J*=3.1 Hz, 2H, coumarin 6,8-*H*), 6.22 (s, 1H, coumarin 3-*H*), 5.56 (d, *J*=5.1 Hz, 1H, O*H*), 4.46 (dd, *J*=7.0, 2.2 Hz, 2H, coumarin-OCH_2), 4.09 (d, *J*=5.0 Hz, 3H, C*H*OH, imidazole-CH_2), 2.41 (s, 3H, coumarin 4-CH_3), 2.39 (d, *J*=6.6 Hz, 2H, CH_2CH$_2$CH$_2$CH$_3$), 1.36 (m, 2H, CH$_2$CH_2CH$_2$CH$_3$), 1.29 (m, 2H, CH$_2$CH$_2$CH_2CH$_3$), 0.89 (t, *J*=7.3 Hz, 3H, CH$_2$CH$_2$CH$_2$CH_3) ppm; ^{13}C NMR (150 MHz, DMSO-d_6) δ: 183.5, 161.8, 160.5, 155.2, 153.7, 151.1, 144.3, 126.9, 122.1, 113.8, 112.8, 111.7, 101.8, 71.7, 67.6, 45.6, 28.8, 26.5, 22.3, 18.5, 14.1 ppm; HRMS (ESI) calcd. for $C_{21}H_{23}ClN_2O_5$ $[M+H]^+$, 419.1374, found, 419.1372.

2.2.7 7-(2-Hydroxy-3-(1*H*-1,2,4-triazol-1-yl)propoxy)-4-methyl-2*H*-chromen-2-one (**5**)

Compound **5** (0.171 g) was obtained as white solid according to general procedure described for **4a** starting from potassium carbonate (0.166 g, 1.2 mmol), 1*H*-1,2,4-triazole (0.069 g, 1 mmol) and compound **3** (0.232 g, 1 mmol). Yield: 56.9%; mp: 144–146 °C; IR (KBr) *v*: 3412 (OH), 3110, 3070 (aromatic C–H), 2952, 2858 (aliphatic C–H), 1708 (C=O), 1621, 1612, 1547, 1513 (aromatic frame), 1393, 1329, 1247, 1187, 1104, 1048, 1009, 982, 745, 687 cm^{-1}; ^1H NMR (300 MHz, DMSO-d_6) δ: 8.48 (s, 1H, triazole 3-*H*), 7.98 (s, 1H, triazole 5-*H*), 7.70 (d, 1H, *J*=3 Hz, coumarin 5-*H*), 7.00 (d, 1H, *J*=3 Hz, coumarin 6-*H*), 6.98 (s, 1H, coumarin 8-*H*), 6.22 (s, 1H, coumarin 3-*H*), 5.57 (s, 1H, O*H*), 4.41–4.28 (m, 2H, phenyl-OCH_2), 4.24–4.21 (m, 1H, C*H*OH), 4.11–4.03 (m, 2H, triazole-CH_2), 2.40 (s, 3H, coumarin 4-CH_3) ppm; ^{13}C NMR (75 MHz, DMSO-d_6) δ: 162.0, 160.8, 155.3, 154.0, 152.0, 145.6, 127.1, 113.9, 113.0, 111.9, 101.9, 70.9, 67.7, 52.4, 18.8 ppm; HRMS (ESI) calcd. for $C_{15}H_{15}N_3O_4$ $[M+H]^+$, 302.1141, found, 302.1148.

2.2.8 7-(2-Hydroxy-3-(1*H*-tetrazol-1-yl)propoxy)-4-methyl-2*H*-chromen-2-one (**6a**)

Compound **6a** (0.638 g) was obtained as white solid according to general procedure described for **4a** starting from potassium carbonate (0.166 g, 1.2 mmol), 1*H*-tetrazole

(0.070 g, 1 mmol) and compound **3** (0.232 g, 1 mmol). Yield: 21.1%; mp: 165–167 °C; IR (KBr) *ν*: 3458 (OH), 3036, 3005 (aromatic C–H), 2967, 2845 (aliphatic C–H), 1721 (C=O), 1600, 1578, 1546, 1501 (aromatic frame), 1274, 1216, 1190, 1169, 1076, 1042, 898, 843 cm^{-1}; ^1H NMR (600 MHz, DMSO-d_6) δ: 9.38 (s, 1H, tetrazole 5-*H*), 7.71 (d, *J*=8.7 Hz, 1H, coumarin 5-*H*), 7.02–6.98 (m, 2H, coumarin 6,8-*H*), 6.23 (s, 1H, coumarin 3-*H*), 5.72 (d, *J*=5.2 Hz, 1H, O*H*), 4.74–4.58 (m, 2H, coumarin-OCH_2), 4.36–4.28 (m, 1H, C*H*OH), 4.11–4.05 (m, 2H, tetrazole-CH_2), 2.41 (s, 3H, coumarin 4-CH_3) ppm; ^{13}C NMR (150 MHz, DMSO-d_6) δ: 161.8, 160.5, 155.1, 153.7, 145.1, 126.9, 113.8, 112.9, 111.7, 101.9, 70.5, 67.4, 51.1, 18.5 ppm; HRMS (ESI) calcd. for $C_{14}H_{14}N_4O_4$ $[M+Na]^+$, 325.0913, found, 325.0916.

2.2.9 7-(2-Hydroxy-3-(5-methyl-1*H*-tetrazol-1-yl) propoxy)-4-methyl-2*H*-chromen-2-one (**6b**)

Compound **6b** (0.135 g) was obtained as white solid according to general procedure described for **4a** starting from potassium carbonate (0.166 g, 1.2 mmol), 5-methyl-1*H*-tetrazole (0.084 g, 1 mmol) and compound **3** (0.232 g, 1 mmol). Yield: 42.6%; mp: 158–160 °C; IR (KBr) *ν*: 3488 (OH), 3076, 3012 (aromatic C–H), 2978, 2812 (aliphatic C–H), 1709 (C=O), 1597, 1585, 1523 (aromatic frame), 1304, 1257, 1212, 1178, 1074, 1012, 890, 863, 762 cm^{-1}; ^1H NMR (600 MHz, DMSO-d_6) δ: 7.71 (d, *J*=8.4 Hz, 1H, coumarin 5-*H*), 7.01 (s, 1H, coumarin 6-*H*), 6.99 (d, *J*=2.4 Hz, 1H, coumarin 8-*H*), 6.23 (s, 1H, coumarin 3-*H*), 5.67 (s, 1H, O*H*), 4.60–4.43 (m, 2H, coumarin-OCH_2), 4.26 (d, *J*=3.6 Hz, 1H, C*H*OH), 4.14–4.10 (m, 2H, tetrazole-CH_2), 2.54 (s, 3H, tetrazole-CH_3), 2.41 (s, 3H, coumarin 4-CH_3) ppm; ^{13}C NMR (150 MHz, DMSO-d_6) δ: 161.8, 160.5, 155.1, 153.7, 153.5, 126.9, 113.9, 112.9, 111.8, 101.9, 70.3, 68.0, 49.9, 18.5, 9.0 ppm; HRMS (ESI) calcd. for $C_{15}H_{16}N_4O_4$ $[M+Na]^+$, 339.1069, found, 339.1072.

2.2.10 7-(3-(1*H*-Benzo[d][1,2,3]triazol-1-yl)-2-hydroxy-propoxy)-4-methyl-2*H*-chromen-2-one (**7a**)

Compound **7a** (0.146 g) was obtained as white solid according to general procedure described for **4a** starting from potassium carbonate (0.166 g, 1.2 mmol), 1*H*-benzo[d][1,2,3]triazole (0.119 g, 1 mmol) and compound **3** (0.232 g, 1 mmol). Yield: 41.5%; mp: 198–200 °C; IR (KBr) *ν*: 3424 (OH), 3097, 3046 (aromatic C–H), 2921, 2853 (aliphatic C–H), 1720 (C=O), 1617, 1586, 1507 (aromatic frame), 1396, 1315, 1306, 1296, 1120, 1036, 990, 940, 827, 786, 712 cm^{-1}; ^1H NMR (300 MHz, DMSO-d_6) δ: 7.95–7.92 (m, 2H, benzotriazole 4,7-*H*), 7.72 (d, 1H, *J*=9 Hz, coumarin 5-*H*), 7.46–7.43 (m, 2H, benzotriazole 5,6-*H*), 6.82–6.78 (m, 2H, coumarin 6,8-*H*), 6.14 (s, 1H, coumarin 3-*H*), 5.91 (s, 1H, O*H*), 4.29–4.20 (m, 2H, phenyl-OCH_2), 3.92–3.48 (m, 3H, C*H*OHCH_2), 2.38 (s, 3H, coumarin 4-CH_3) ppm; ^{13}C NMR (75 MHz, DMSO-d_6) δ: 161.6, 160.2, 155.8, 153.7, 146.9, 137.0, 124.5, 119.4, 117.3, 110.8, 112.5, 111.6, 111.3, 102.3, 71.9, 66.8, 45.7, 18.8 ppm; HRMS (ESI) calcd. for $C_{19}H_{17}N_3O_4$ $[M+H]^+$, 352.1297, found, 352.1294.

2.2.11 7-(2-Hydroxy-3-(5-methyl-1*H*-benzo[d][1,2,3]triazol-1-yl)propoxy)-4-methyl-2*H*-chromen-2-one (**7b**)

Compound **7b** (0.305 g) was obtained as white solid according to general procedure described for **4a** starting from potassium carbonate (0.166 g, 1.2 mmol), 5-methyl-1*H*-benzo[d][1,2,3]triazole (0.133 g, 1 mmol) and compound **3** (0.232 g, 1 mmol). Yield: 83.6%; mp: 80–82 °C; IR (KBr) *ν*: 3478 (OH), 3095, 3021 (aromatic C–H), 2978, 2865 (aliphatic C–H), 1719 (C=O), 1596, 1584, 1523, 1469 (aromatic frame), 1304, 1296, 1243, 1117, 1085, 1032, 886, 856, 762 cm^{-1}; ^1H NMR (600 MHz, DMSO-d_6) δ: 7.89 (d, *J*=8.5 Hz, 1H, benzotriazole 7-*H*), 7.77 (d, *J*=13.6 Hz, 1H, coumarin 5-*H*), 7.71 (s, 1H, benzotriazole 4-*H*), 7.21 (d, *J*=8.5 Hz, 1H, benzotriazole 6-*H*), 6.99 (dd, *J*=6.9, 4.4 Hz, 2H, coumarin 6,8-*H*), 6.22 (s, 1H, coumarin 3-*H*), 5.58 (s, 1H, O*H*), 4.88–4.76 (m, 2H, coumarin-OCH_2), 4.38 (s, 1H, C*H*OH), 4.14–4.06 (m, 2H, benzotriazole-CH_2), 2.46 (s, 3H, benzotriazole 5-CH_3), 2.40 (s, 3H, coumarin 4-CH_3) ppm; ^{13}C NMR (150 MHz, DMSO-d_6) δ: 161.9, 160.5, 155.1, 153.7, 144.2, 134.6, 132.8, 129.5, 126.9, 126.3, 113.8, 112.8, 111.7, 111.1, 101.9, 70.6, 68.3, 50.9, 21.8, 18.5 ppm; HRMS (ESI) calcd. for $C_{20}H_{19}N_3O_4$ $[M+Na]^+$, 388.1273, found, 388.1276.

2.2.12 7-(2-Hydroxy-3-(1-methyl-1*H*-imidazol-2-ylthio) propoxy)-4-methyl-2*H*-chromen-2-one (**8**)

Compound **8** (0.208 g) was obtained as white solid according to general procedure described for **4a** starting from potassium carbonate (0.166 g, 1.2 mmol), 1-methyl-1*H*-imidazole-2-thiol (0.114 g, 1 mmol) and compound **3** (0.232 g, 1 mmol). Yield: 60.1%; mp: 145–147 °C; IR (KBr) *ν*: 3488 (OH), 3086, 3021 (aromatic C–H), 2986, 2847 (aliphatic C–H), 1716 (C=O), 1602, 1596, 1569, 1501 (aromatic frame), 1274, 1206, 1179, 1159, 1064, 1003, 898, 858, 780 cm^{-1}; ^1H NMR (600 MHz, DMSO-d_6) δ: 7.68 (d, *J*=9.2 Hz, 1H, coumarin 5-*H*), 7.23 (d, *J*=8.5 Hz, 1H, imidazole 4-*H*), 6.97 (m, 2H, coumarin 6,8-*H*), 6.92 (d, *J*=5.2 Hz, 1H, imidazole 5-*H*), 6.21 (s, 1H, coumarin 3-*H*), 5.78 (s, 1H, O*H*), 4.13–4.04 (m, 3H, coumarin-OCH_2, C*H*OH), 3.59 (s, 3H, imidazole 1-CH_3), 3.25–3.15 (m, 2H, imidazole-CH_2), 2.40 (s, 3H, coumarin 4-CH_3) ppm; ^{13}C NMR (150 MHz, DMSO-d_6) δ: 162.1, 160.5, 155.1, 153.8, 141.0, 128.6, 126.8, 123.6, 113.6, 112.9, 111.6, 101.8, 71.8, 68.6, 37.5, 33.3, 18.5 ppm; HRMS (ESI) calcd. for $C_{17}H_{18}N_2O_4S$ $[M+H]^+$, 347.1066, found, 347.1065, $[M+Na]^+$, 369.0885, found, 369.0888.

2.2.13 7-(3-(1*H*-1,2,4-Triazol-3-ylthio)-2-hydroxy-propoxy)-4-methyl-2*H*-chromen-2-one (**9**)

Compound **9** (0.092 g) was obtained as yellow solid according to general procedure described for **4a** starting from potassium carbonate (0.166 g, 1.2 mmol), 1*H*-1,2,4-tria-

zole-3-thiol (0.101 g, 1 mmol) and compound **3** (0.232 g, 1 mmol). Yield: 27.6%; mp: 46–48 °C; IR (KBr) *v*: 3465 (OH), 3295 (NH), 3098, 3042 (aromatic C–H), 2997, 2865 (aliphatic C–H), 1715 (C=O), 1586, 1564, 1523 (aromatic frame), 1304, 1277, 1236, 1159, 1064, 1031, 859, 814, 798 cm^{-1}; ^1H NMR (600 MHz, DMSO-d_6) δ: 8.40 (s, 1H, triazole 5-*H*), 7.68 (d, *J*=8.5 Hz, 1H, coumarin 5-*H*), 7.01–6.91 (m, 2H, coumarin 6,8-*H*), 6.21 (s, 1H, coumarin 3-*H*), 4.17–4.06 (m, 3H, coumarin-OCH_2, C*H*OH), 3.36–3.26 (m, 2H, triazole-CH_2), 2.40 (s, 3H, coumarin 4-CH_3) ppm; ^{13}C NMR (150 MHz, DMSO-d_6) δ: 162.1, 160.5, 155.1, 153.7, 126.8, 113.7, 112.8, 111.6, 101.8, 71.8, 68.3, 46.8, 18.5 ppm; HRMS (ESI) calcd. for $C_{15}H_{15}N_3O_4S$ $[M+H]^+$, 334.0862, found, 334.0863, $[M+Na]^+$, 356.0681, found, 356.0680.

2.2.14 5,7-Bis(2-hydroxy-3-(1H-imidazol-1-yl)propoxy)-4-methyl-2H-chromen-2-one (**13a**)

Compound **13a** (0.118 g) was obtained as white solid according to general procedure described for **4a** starting from potassium carbonate (0.332 g, 2.4 mmol), 1*H*-imidazole (0.136 g, 2 mmol) and compound **12** (0.304 g, 1 mmol). Yield: 26.8%; mp: 78–80 °C; IR (KBr) *v*: 3485 (OH), 3086, 3012 (aromatic C–H), 2987, 2865 (aliphatic C–H), 1721 (C=O), 1570, 1564, 1531, 1487 (aromatic frame), 1297, 1264, 1176, 1159, 1025, 1001, 879, 864, 795 cm^{-1}; ^1H NMR (600 MHz, DMSO-d_6) δ: 7.75 (s, 2H, imidazole 2-*H*), 7.23 (d, *J*=4.8 Hz, 2H, idaimzole 4-*H*), 6.97 (d, *J*=4.6 Hz, 2H, idaimzole 5-*H*), 6.57 (d, *J*=2.2 Hz, 2H, coumarin 6,8-*H*), 6.01 (s, 1H, coumarin 3-*H*), 4.25–4.07 (m, 6H, coumarin-OCH_2, C*H*OH), 4.02–3.96 (m, 4H, imidazole-CH_2), 2.55 (s, 3H, coumarin 4-CH_3) ppm; ^{13}C NMR (150 MHz, DMSO-d_6) δ: 162.2, 160.1, 158.8, 156.7, 154.8, 138.1, 127.7, 120.8, 111.2, 104.7, 96.9, 94.8, 72.0, 66.4, 49.8, 24.3 ppm; HRMS (ESI) calcd. for $C_{22}H_{24}N_4O_6$ $[M+H]^+$, 441.1774, found, 441.1773.

2.2.15 5,7-Bis(2-hydroxy-3-(2-phenyl-1H-imidazol-1-yl)propoxy)-4-methyl-2H-chromen-2-one (**13b**)

Compound **13b** (0.164 g) was obtained as white solid according to general procedure described for **4a** starting from potassium carbonate (0.332 g, 2.4 mmol), 2-phenyl-1*H*-imidazole (0.288 g, 2 mmol) and compound **12** (0.304 g, 1 mmol). Yield: 27.6%; mp: 44–46 °C; IR (KBr) *v*: 3464 (OH), 3096, 3015 (aromatic C–H), 2979, 2842 (aliphatic C–H), 1727 (C=O), 1607, 1587, 1554, 1510 (aromatic frame), 1287, 1278, 1176, 1126, 1076, 1042, 878, 854 cm^{-1}; ^1H NMR (600 MHz, DMSO-d_6) δ: 7.68–7.62 (m, 4H, phenyl 2,6-*H*), 7.47 (dd, *J*=15.5, 6.2 Hz, 6H, phenyl 2,6-*H*), 7.40–7.39 (m, 2H, idaimzole 4-*H*), 7.17 (d, *J*=3.9 Hz, 2H, imidazole 5-*H*), 6.56–6.47 (m, 2H, coumarin 6,8-*H*), 6.02 (s, 1H, coumarin 3-*H*), 5.65 (s, 2H, O*H*), 4.30–4.14 (m, 6H, coumarin-OCH_2, C*H*OH), 4.06–3.94 (m, 4H, imidazole-CH_2), 2.56 (s, 3H, coumarin 4-CH_3) ppm; ^{13}C NMR (150 MHz, DMSO-d_6) δ: 161.9, 160.1, 158.8, 158.3, 156.7, 154.7, 147.4, 129.4, 128.9, 128.8, 122.8, 122.6, 111.2, 104.4, 96.7, 94.9, 71.8, 68.5, 49.8, 24.3 ppm; HRMS (ESI) calcd. for $C_{34}H_{32}N_4O_6$ $[M+H]^+$, 593.2400, found, 593.2401.

2.2.16 5,7-Bis(2-hydroxy-3-(2-methyl-5-nitro-1H-imidazol-1-yl)propoxy)-4-methyl-2H-chromen-2-one (**13c**)

Compound **13c** (0.456 g) was obtained as yellow solid according to general procedure described for **4a** starting from potassium carbonate (0.332 g, 2.4 mmol), 2-methyl-5-nitro-1*H*-imidazole (0.254 g, 2 mmol) and compound **12** (0.304 g, 1 mmol). Yield: 81.7%; mp: 199–201 °C; IR (KBr) *v*: 3428 (OH), 3122, 3051 (aromatic C–H), 2924, 2853 (aliphatic C–H), 1719 (C=O), 1619, 1564, 1508, 1463 (aromatic frame), 1431, 1383, 1275, 1187, 1118, 1041, 1002, 959, 834, 739 cm^{-1}; ^1H NMR (300 MHz, DMSO-d_6) δ: 8.32 (d, 2H, *J*=9 Hz, imidazole 4-*H*), 6.67 (s, 1H, coumarin 8-*H*), 6.55 (s, 1H, coumarin 6-*H*), 6.07 (s, 1H, coumarin 3-*H*), 5.67 (s, 2H, O*H*), 4.26–4.21 (m, 4H, phenyl-OCH_2), 4.11–4.04 (m, 6H, C*H*OHCH_2), 2.61 (s, 3H, coumarin 4-CH_3), 2.39 (s, 6H, imidazole 2-CH_3) ppm; ^{13}C NMR (75 MHz, DMSO-d_6) δ: 162.0, 160.0, 158.4, 156.7, 154.7, 146.1, 145.7, 123.3, 111.3, 104.7, 97.1, 95.0, 71.4, 70.5, 68.2, 50.2, 24.5, 13.2 ppm; HRMS (ESI) calcd. for $C_{24}H_{26}N_6O_{10}$ $[M+H]^+$, 559.1789, found, 559.1788.

2.2.17 5,7-Bis(2-hydroxy-3-(4-nitro-1H-imidazol-1-yl)propoxy)-4-methyl-2H-chromen-2-one (**13d**)

Compound **13d** (0.463 g) was obtained as yellow solid according to general procedure described for **4a** starting from potassium carbonate (0.332 g, 2.4 mmol), 4-nitro-1*H*-imidazole (0.226 g, 2 mmol) and compound **12** (0.304 g, 1 mmol). Yield: 87.2%; mp: 220–221 °C; IR (KBr) *v*: 3413 (OH), 3166, 3062 (aromatic C–H), 2923, 2850 (aliphatic C–H), 1707 (C=O), 1617, 1613, 1576, 1510 (aromatic frame), 1379, 1282, 1206, 1154, 1088, 1010, 970, 851, 782 cm^{-1}; ^1H NMR (300 MHz, DMSO-d_6) δ: 8.29 (s, 1H, imidazole 5-*H*), 7.96 (s, 1H, imidazole 2-*H*), 6.69 (s, 1H, coumarin 8-*H*), 6.54 (s, 1H, coumarin 6-*H*), 6.12 (s, 1H, coumarin 3-*H*), 5.65 (s, 2H, O*H*), 4.29–4.23 (m, 4H, phenyl-OCH_2), 4.15–4.06 (m, 6H, C*H*OHCH_2), 2.41 (s, 3H, coumarin 4-CH_3) ppm; ^{13}C NMR (75 MHz, DMSO-d_6) δ: 162.3, 160.2, 157.8, 156.1, 154.2, 147.7, 140.5, 128.4, 110.6, 104.3, 97.5, 95.3, 71.4, 70.8, 68.1, 49.9, 24.3 ppm; HRMS (ESI) calcd. for $C_{22}H_{22}N_6O_{10}$ $[M+H]^+$, 531.1476, found, 531.1478.

2.2.18 1,1′-(3,3′-(4-Methyl-2-oxo-2H-chromene-5,7-diyl)bis(oxy)bis(2-hydroxypropane-3,1-diyl))bis(2-butyl-4-chloro-1H-imidazole-5-carbaldehyde) (**13e**)

Compound **13e** (0.159 g) was obtained as yellow solid according to general procedure described for **4a** starting from potassium carbonate (0.332 g, 2.4 mmol), 2-butyl-4-chloro-1*H*-imidazole-5-carbaldehyde (0.373 g, 2 mmol) and compound **12** (0.304 g, 1 mmol). Yield: 23.5%; mp: 92–94 °C; IR (KBr) *v*: 3454 (OH), 3076, 3031 (aromatic C–H), 2970, 2856 (aliphatic C–H), 1705 (C=O), 1574,

1546, 1497 (aromatic frame), 1297, 1265, 1201, 1186, 1064, 1001, 887, 843 cm^{-1}; ^1H NMR (600 MHz, DMSO-d_6) δ: 9.67 (s, 1H, C*H*O), 9.61 (s, 1H, C*H*O), 6.61 (s, 1H, coumarin 8-*H*), 6.52 (s, 1H, coumarin 6-*H*), 6.06 (s, 1H, coumarin 3-*H*), 5.55 (t, *J*=19.3 Hz, 2H, O*H*), 4.51–3.93 (m, 10H, coumarin-OCH_2, C*H*OH, imidazole-CH_2), 2.79–2.61 (m, 7H, CH_2CH_2CH_2CH, coumarin 4-CH_3), 1.67 (dd, *J*=7.5, 2.9 Hz, 4H, CH$_2$CH_2CH$_2$CH$_3$), 1.36–1.29 (m, 4H, CH$_2$CH$_2$CH_2CH$_3$), 0.90 (t, *J*=7.3 Hz, 6H, CH$_2$CH$_2$CH$_2$CH_3) ppm; ^{13}C NMR (150 MHz, DMSO-d_6) δ: 178.1, 162.0, 160.0, 158.6, 156.7, 155.4, 154.6, 144.3, 124.5, 111.3, 104.7, 96.8, 95.1, 71.7, 68.3, 46.0, 29.0, 26.1, 24.4, 22.3, 14.1 ppm; HRMS (ESI) calcd. for $C_{32}H_{38}Cl_2N_4O_8$ $[M+H]^+$, 677.2145, found, 677.2146.

2.2.19 5,7-Bis(2-hydroxy-3-(1*H*-1,2,4-triazol-1-yl) propoxy)-4-methyl-2*H*-chromen-2-one (**14**)

Compound **14** (0.257 g) was obtained as white solid according to general procedure described for **4a** starting from potassium carbonate (0.332 g, 2.4 mmol), 1*H*-1,2,4-triazole (0.138 g, 2 mmol) and compound **12** (0.304 g, 1 mmol). Yield: 58.0%; mp: 188–190 °C; IR (KBr) ν: 3418 (OH), 3109, 3064 (aromatic C–H), 2962, 2868 (aliphatic C–H), 1713 (C=O), 1624, 1602, 1507, 1465 (aromatic frame), 1392, 1379, 1287, 1207, 1154, 1092, 1019, 962, 865 cm^{-1}; ^1H NMR (300 MHz, DMSO-d_6) δ: 8.50 (d, 2H, *J*=6 Hz, triazole 3-*H*), 8.00 (d, 2H, *J*=3 Hz, triazole 5-*H*), 6.60 (s, 1H, coumarin 8-*H*), 6.50 (s, 1H, coumarin 6-*H*), 6.04 (s, 1H, coumarin 3-*H*), 5.59–5.56 (d, 1H, *J*=9 Hz, O*H*), 4.42–4.21 (m, 6H, coumarin-OCH_2 C*H*OH), 4.11–4.00 (m, 4H, triazole-CH_2), 2.59 (s, 3H, coumarin 4-CH_3) ppm; ^{13}C NMR (75 MHz, DMSO-d_6) δ: 162.1, 160.1, 158.5, 156.7, 154.8, 151.8, 145.3, 111.3, 104.7, 97.0, 94.8, 71.3, 70.6, 67.6, 52.5, 24.4 ppm; HRMS (ESI) calcd. for $C_{20}H_{22}N_6O_6$ $[M+H]^+$, 443.1679, found, 443.1680.

2.2.20 5,7-Bis(2-hydroxy-3-(1*H*-tetrazol-1-yl)propoxy)-4-methyl-2*H*-chromen-2-one (**15a**)

Compound **15a** (0.091 g) was obtained as white solid according to general procedure described for **4a** starting from potassium carbonate (0.332 g, 2.4 mmol), 1*H*-tetrazole (0.140 g, 2 mmol)and compound **12** (0.304 g, 1 mmol). Yield: 20.6%; mp: 106–108 °C; IR (KBr) ν: 3475 (OH), 3076, 3033 (aromatic C–H), 2982, 2863 (aliphatic C–H), 1714 (C=O), 1596, 1578, 1525, 1503 (aromatic frame), 1314, 1296, 1275, 1179, 1063, 1025, 888, 844 cm^{-1}; ^1H NMR (600 MHz, DMSO-d_6) δ: 9.31 (s, 2H, tetrazole 5-*H*), 6.56 (s, 1H, coumarin 8-*H*), 6.50 (s, 1H, coumarin 6-*H*), 6.03 (s, 1H, coumarin 3-*H*), 5.79 (d, *J*=5.2 Hz, 2H, O*H*), 4.75–4.22 (m, 6H, coumarin-OCH_2 C*H*OH), 4.16–4.08 (m, 4H, tetrazole-CH_2), 2.56 (s, 3H, coumarin 4-CH_3) ppm; ^{13}C NMR (150 MHz, DMSO-d_6) δ: 162.8, 160.9, 155.6, 153.4, 145.7, 126.9, 113.8, 112.8, 111.5, 101.3, 70.5, 67.8, 51.3, 18.6 ppm; HRMS (ESI) calcd. for $C_{18}H_{20}N_8O_6$ $[M+H]^+$, 445.1584, found, 445.1586.

2.2.21 5,7-Bis(2-hydroxy-3-(5-methyl-1*H*-tetrazol-1-yl) propoxy)-4-methyl-2*H*-chromen-2-one (**15b**)

Compound **15b** (0.136 g) was obtained as white solid according to general procedure described for **4a** starting from potassium carbonate (0.332 g, 2.4 mmol), 5-methyl-1*H*-tetrazole (0.168 g, 2 mmol) and compound **12** (0.304 g, 1 mmol). Yield: 28.8%; mp: 115–117 °C; IR (KBr) ν: 3437 (OH), 3075, 3026 (aromatic C–H), 2971, 2852 (aliphatic C–H), 1730 (C=O), 1598, 1574, 1538 (aromatic frame), 1242, 1185, 1174, 1102, 1085, 1024, 879, 864 cm^{-1}; ^1H NMR (600 MHz, DMSO-d_6) δ: 6.64 (s, 1H, coumarin 8-*H*), 6.55 (s, 1H, coumarin 6-*H*), 6.05 (s, 1H, coumarin 3-*H*), 5.67 (s, 2H, O*H*), 4.80–4.27 (m, 6H, phenyl-OCH_2 C*H*OH), 4.19–4.03 (m, 4H, tetrazole-CH_2), 2.55 (s, 3H, coumarin 4-CH_3), 2.46 (s, 6H, tetrazole-CH_3) ppm; ^{13}C NMR (150 MHz, DMSO-d_6) δ: 162.0, 160.0, 158.4, 156.8, 154.6, 153.5, 111.4, 104.8, 97.1, 95.0, 70.3, 68.0, 49.9, 24.3, 10.9 ppm; HRMS (ESI) calcd. for $C_{20}H_{24}N_8O_6$ $[M+H]^+$, 473.1897, found, 473.1899.

2.2.22 5,7-Bis(3-(1*H*-benzo[d][1,2,3]triazol-1-yl)-2-hydroxypropoxy)-4-methyl-2*H*-chromen-2-one (**16a**)

Compound **16a** (0.224 g) was obtained as white solid according to general procedure described for **4a** starting from potassium carbonate (0.332 g, 2.4 mmol), 1*H*-benzo[d][1,2,3]triazole (0.238 g, 2 mmol) and compound **12** (0.304 g, 1 mmol). Yield: 41.2%; mp: 214–216 °C; IR (KBr) ν: 3417 (OH), 3107, 3078 (aromatic C–H), 2928, 2859 (aliphatic C–H), 1710 (C=O), 1628, 1601, 1565, 1515 (aromatic frame), 1438, 1411, 1380, 1246, 1124, 1029, 940, 833, 763 cm^{-1}; ^1H NMR (300 MHz, DMSO-d_6) δ: 7.95 (d, 2H, *J*=9 Hz, benzotriazole 4-*H*), 7.72 (d, 2H, *J*=6 Hz, benzotriazole 7-*H*), 7.44 (m, 4H, benzotriazole 5,6-*H*), 6.52 (s, 1H, coumarin 6-*H*), 6.47 (s, 1H, coumarin 8-*H*), 6.04 (s, 1H, coumarin 3-*H*), 5.55 (s, 2H, O*H*), 4.39–4.31 (m, 4H, phenyl-OCH_2), 4.13–3.95 (m, 6H, C*H*OHCH_2), 2.42 (s, 3H, coumarin 4-CH_3) ppm; ^{13}C NMR (75 MHz, DMSO-d_6) δ: 162.2, 160.4, 158.4, 156.6, 155.3, 145.9, 133.0, 119.6, 116.3, 110.5, 112.5, 110.9, 97.3, 95.3, 71.9, 70.9, 66.8, 46.7, 20.8 ppm; HRMS (ESI) calcd. for $C_{28}H_{26}N_6O_6$ $[M+H]^+$, 543.1992, found, 543.1994.

2.2.23 5,7-Bis(2-hydroxy-3-(5-methyl-1*H*-benzo[d][1,2,3]triazol-1-yl)propoxy)-4-methyl-2*H*-chromen-2-one (**16b**)

Compound **16b** (0.237 g) was obtained as white solid according to general procedure described for **4a** starting from potassium carbonate (0.332 g, 2.4 mmol), 5-methyl-1*H*-benzo[d][1,2,3]triazole (0.266 g, 2 mmol) and compound **12** (0.304 g, 1 mmol). Yield: 41.6%; mp: 89–91 °C; IR (KBr) ν: 3495 (OH), 3069, 3005 (aromatic C–H), 2968, 2854 (aliphatic C–H), 1713 (C=O), 1604, 1594, 1566, 1517 (aromatic frame), 1294, 1281, 1186, 1159, 1032, 1007, 897, 846 cm^{-1}; ^1H NMR (600 MHz, DMSO-d_6) δ: 7.79 (d,

J=3.2 Hz, 2H, benzotriazole 7-*H*), 7.66 (s, 2H, benzotriazole 4-*H*), 7.26 (d, *J*=8.7 Hz, 2H, benzotriazole 6-*H*), 6.59 (s, 1H, coumarin 8-*H*), 6.50 (s, 1H, coumarin 6-*H*), 6.03 (s, 1H, coumarin 3-*H*), 5.58 (s, 2H, O*H*), 4.91–4.75 (m, 4H, coumarin-OCH_2), 4.14 (m, 2H, C*H*OH), 4.09–3.45 (m, 4H, benzotriazole-CH_2), 2.62 (s, 3H, coumarin 4-CH_3), 2.45 (s, 6H, benzotriazole 5-CH_3) ppm; ^{13}C NMR (150 MHz, DMSO-d_6) δ: 162.1, 160.0, 158.5, 156.7, 154.7, 144.7, 136.3, 132.8, 129.4, 126.3, 117.7, 116.4, 111.4, 97.1, 95.0, 68.4, 66.4, 59.3, 24.4, 21.9 ppm; HRMS (ESI) calcd. for $C_{30}H_{30}N_6O_6$ $[M+H]^+$, 571.2305, found, 571.2310, $[M+Na]^+$, 593.2125, found, 593.2126.

2.2.24 5,7-Bis(2-hydroxy-3-(1-methyl-1*H*-imidazol-2-ylthio)propoxy)-4-methyl-2*H*-chromen-2-one (**17**)

Compound **17** (0.320 g) was obtained as white solid according to general procedure described for **4a** starting from potassium carbonate (0.332 g, 2.4 mmol), 1-methyl-1*H*-imidazole-2-thiol (0.228 g, 2 mmol) and compound **12** (0.304 g, 1 mmol). Yield: 60.1%; mp: 42–44 °C; IR (KBr) ν: 3464 (OH), 3062, 3015 (aromatic C–H), 2967, 2860 (aliphatic C–H), 1721 (C=O), 1594, 1586, 1543, 1458 (aromatic frame), 1275, 1216, 1161, 1159, 1032, 1021, 887, 847 cm^{-1}; ^{1}H NMR (600 MHz, DMSO-d_6) δ: 7.22 (d, *J*=6.4 Hz, 2H, imidazole 4-*H*), 6.92 (d, *J*=12.8 Hz, 2H, imidazole 5-*H*), 6.55–6.47 (d, *J*=2.2 Hz, 2H, coumarin 6,8-*H*), 5.99 (s, 1H, coumarin 3-*H*), 4.11–4.06 (m, 6H, coumarin-OCH_2, C*H*OH), imidazole-CH_2), 2.52 (s, 3H, coumarin 4-CH_3) ppm; ^{13}C NMR (150 MHz, DMSO-d_6) δ: 162.3, 160.1, 158.6, 156.7, 154.8, 141.0, 128.6, 123.6, 111.1, 104.6, 96.9, 94.9, 71.7, 68.6, 37.5, 33.4, 24.3 ppm; HRMS (ESI) calcd. for $C_{24}H_{28}N_4O_6S_2$ $[M+H]^+$, 533.1529, found, 533.1532, $[M+Na]^+$, 555.1348, found, 555.1343.

2.3 Biological assays

The *in vitro* MIC of the target compounds were determined using the two-fold serial dilution technique in 96-well microtest plates, according to the National Committee for Clinical Laboratory Standards (NCCLS) [25]. The tested microorganism strains were provided by the School of Pharmaceutical Sciences, Southwest University and the College of Pharmacy, Third Military Medical University, China. Chloramphenicol, Norfloxacin and Fluconazole were used as standard drugs.

2.3.1 Antibacterial assays

The prepared compounds **4**–**9** and **13**–**17** were evaluated for their antibacterial activities against Gram-positive bacteria (*Methicillin-resistant Staphylococcus aureus* N315 (MRSA), *B. subtilis* ATCC 21216 and *M. luteus* ATCC 4698), and Gram-negative bacteria (*E. coli* JM 109, *P. aeruginosa* ATCC 27853 and *S. dysenteriae*). The bacterial suspension was adjusted with sterile saline to a concentration of 1×10^5 CFU. The tested compounds were dissolved in DMSO to prepare the stock solutions. The tested compounds and reference drugs were prepared in Mueller-Hinton broth (Guangdong Huaikai Microbial Sci & Tech Co., Ltd., China) by two-fold serial dilution to give the required concentrations of 512, 256, 128, 64, 32, 16, 8, 4, 2, 1, and 0.5 μg/mL. These dilutions were inoculated and incubated at 37 °C for 24 h. To ensure that the solvent had no effect on bacterial growth, a control test was performed with test medium supplemented with DMSO at the same dilutions used in the experiment.

2.3.2 Antifungal assays

The newly synthesized compounds **4**–**9** and **13**–**17** were evaluated for their antifungal activities against *C. albicans* ATCC 76615, *B. yeast*, *C. utilis*, *C. mycoderma* and *A. flavus*. A spore suspension in sterile distilled water was prepared from a culture of the fungi growing on Sabouraud agar (SA) media, aged 1 d. The final spore concentration was 1×10^3–5×10^3 spore/mL. From the stock solutions of the tested compounds and reference antifungal drug Fluconazole, dilutions in sterile RPMI 1640 medium (Neuronbc Laboraton Technology CO., Ltd., China) were made, resulting in eleven desired concentrations (0.5 to 512 μg/mL) of each tested compound. These dilutions were inoculated and incubated at 35 °C for 24 h.

2.3.3 logP_{ow} values

The partition coefficient (*P*) is defined as the ratio of the equilibrium concentrations of a dissolved substance in a two-phase system (*n*-octanol and water), which are two largely immiscible solvents. Octanol represents a substitute for biotic lipid and hence gives an approximation to a biotic lipid-water partition coefficient. The ratio is reported as a logarithm usually as logP_{ow} or logK_{ow}. In this paper, we employed the traditional saturation shake flask approach and UV-Vis spectrophotometric methods to measure the values of logP_{ow} (Supporting Information online).

3 Results and discussion

3.1 Chemistry

The choice of base in the preparation of intermediates **3** and **12** was important, and results showed that potassium carbonate was the best choice. The amount of 2-(chloromethyl)oxirane was another key factor when the synthesis of compounds **3** and **12**. In this reaction, 2-(chloromethyl)oxirane acted as not only reactant but also solvent, the optimal ratio of hydroxyl coumarin, potassium carbonate and 2-(chloromethyl)oxirane was 1:1.2:20. For the synthesis of target compounds, the effect of reaction temperature was quite remarkable. Take 2-methyl-5-nitro-1*H*-imidazole as an example, it could generate tautomeric interconversion under basic conditions (Figure 2). In the pre-

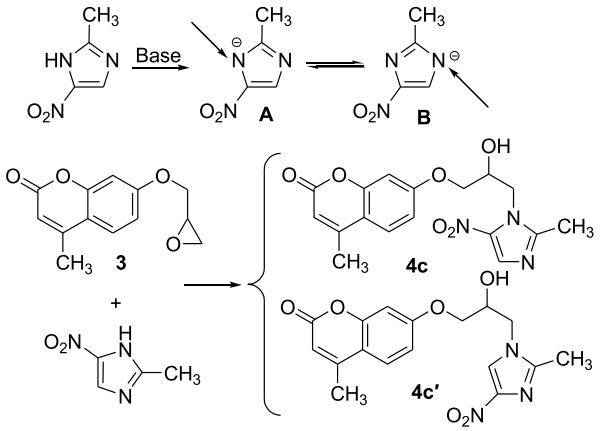

Figure 2 Reaction of compound **3** with 2-methyl-5-nitro-1*H*-imidazole.

sence of potassium carbonate, 2-methyl-5-nitro-1*H*-imidazole gives two stable resonance forms **A** and **B**, accordingly two products **4c** and **4c′** could be yielded. The experimental exploration suggested that the optimal reaction temperature was 70 °C.

3.2 Spectral analysis

All the newly synthesized target coumarin azoles were characterized by IR, ^{1}H NMR, ^{13}C NMR and HRMS spectra. The spectral analyses were in accordance with the assigned structures, and all the spectral data were listed in the experimental section.

3.2.1 IR spectra

Almost all the target compounds gave similar IR spectra and there is no large difference for the characteristic absorption peaks. In IR spectra, coumarin mono-azoles **4**–**9** and bis-azoles **13**–**17** gave a broad absorption in 3495–3408 cm^{-1} and sharp peaks in 1247–1001 cm^{-1} which indicated the presence of secondary alcohol. The aryl characteristic C–H bands appeared in the region between 3166 and 3005 cm^{-1} as well as the stretching vibrations of aromatic frame peaks at 1628–1458 cm^{-1}, while the absorption bands ascribed to aliphatic C–H stretching vibrations were seen at two regions of 2997–2921 and 2868–2812 cm^{-1}. The stretching vibrations of C=O bonds in target compounds were observed at 1730–1705 cm^{-1}. Furthermore, moderate absorption bands at 3295 cm^{-1} in compound **9** was attributed to the stretching vibration of N–H bond. All the other absorption bands were also observed at expected regions.

3.2.2 ^{1}H NMR spectra

In ^{1}H NMR spectra, all the protons in coumarin skeleton for the same series of target compounds showed no remarkable signal change when azoles were introduced. However, due to the influence of different azoles, some ^{1}H NMR data such as H^a exhibited downfield signals. Table 1 clearly showed that

Table 1 Some ^{1}H NMR data (δ(ppm)) of compounds **4a**, **5**, **6a**, **13a**, **14** and **15a**

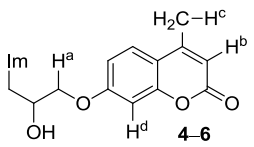

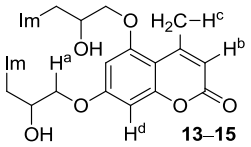

Compounds	Im	H^a	H^b	H^c	H^d
4a	Imidazolyl	4.19−4.11	6.22	2.40	6.99
13a	Imidazolyl	4.25−4.17	6.01	2.55	6.57
5	Triazolyl	4.41−4.28	6.22	2.40	6.98
14	Triazolyl	4.42−4.30	6.04	2.59	6.60
6a	Tetrazolyl	4.74−4.58	6.23	2.41	6.98
15a	Tetrazolyl	4.75−4.56	6.03	2.56	6.56

the chemical shifts of H^a followed the order: **6a/15a**> **5/14**>**4a/13a**, which indicated that the electronegativity order of azole ring should be tetrazole>triazole>imidazole. For mono-azole ethanols **4**–**9** and bis-azole ones **13**–**17**, the number of azole ring had large effects on chemical shifts for some protons in coumarin skeleton. For example, proton H^b of compound **13a** appeared a singlet at δ 6.01 ppm, which displayed approximately 0.2 ppm upfield shift compared to **4a**, and the proton H^c in bis-azole ethanol **14** displayed downfield shift at δ 2.59 ppm in comparison with mono-azole ethanol **5** (δ 2.40 ppm), which was probably due to the electron-withdrawing character of the substituent at 5-position in coumarin ring. In addition, upfield chemical shift at δ 6.56 ppm was observed for proton H^d in compound **15a** in comparison with mono-tetrazolyl ethanol **6a** (δ 6.98 ppm). For all these observations, the introduction and the number of azole ring were the main factor effecting ^{1}H chemical shifts.

3.2.3 ^{13}C NMR spectra

The ^{13}C NMR spectra of all the compounds were in accordance with the assigned structures. No large difference was found in ^{13}C chemical shifts for compounds **4**–**9** and **13**–**17**, respectively. While in comparison **4**–**9** with **13**–**17**, except for 5- and 6-position, there were nearly the same ^{13}C chemical shifts in coumarin skeleton. The substitution by strong electrophilic groups in compounds **13**–**17** resulted in downfield ^{13}C chemical shifts with 158.3–153.4 ppm for the C-5 position in comparison with compounds **4**–**9** (127.1–124.5 ppm). The signals observed at δ 111.9–110.3 ppm in coumarins **4**–**9** at 6-position exhibited larger downfield shifts than that in compounds **13**–**17** (δ 97.8–97.0 ppm) due to the synergetic influence of substituents at C-5 and C-7 positions.

3.3 Biological activity

3.3.1 Antibacterial activity

The antibacterial tests showed that some of the prepared compounds exhibited moderate to good efficacy against all the

tested bacterial strains, especially compound **14** displayed remarkable antibacterial activities in comparison with the reference drugs Chloramphenicol and Norfloxacin, which indicated that compound **14** could be employed to further study as novel potential antimicrobial agent.

Results in Table 2 demonstrated the significant effects of different azole rings on biological activities. Triazolyl moiety modified coumarins **5** and **14** possessed the better antibacterial activities to all the tested strains. Mono-triazolyl ethanol coumarin **5** gave the strongest antibacterial potency against *P. aeruginosa* with MIC value of 4 μg/mL, which was 4- and 8-fold more active than Norfloxacin and Chloramphenicol. Notably, compound **14** with bis-triazolyl ethanol group displayed equivalent and superior anti-MRSA potency (MIC=8 μg/mL) to Norfloxacin (MIC=8 μg/mL) and Chloramphenicol (MIC=16 μg/mL). Regretfully, almost all the coumarin-derived imidazolyl ethanols **4a**–**4c**, **4e** and **13a**–**13e** were unfavorable for the antibacterial efficiency except for mono-4-nitroimidazole ethanol **4d**. This might be explained by their high hydrophobicity, making it difficult to penetrate the cellular membrane and therefore confined the antibacterial activity.

In comparison mono-azolyl ethanol coumarins with bis-azolyl ethanol ones, it was obvious that the activities of mono-azolyl ethanols were better generally. For bis-azolyl ethanols, only compounds **14** and **16a** displayed moderate to good antibacterial efficiency. Among the fused triazolyl ethanol derivatives **7a**–**7b** and **16a**–**16b**, compounds **7a** and **16a** gave comparable inhibitory potency to Chloramphenicol against some tested bacterial strains, whereas methyl-substituted benzotriazolyl coumarins **7b** and **16b** gave lower efficacy against all these strains. This manifested that electron-donating group was unfavorable for the antibacterial efficiency in this type of compounds.

3.3.2 Antifungal activity

The *in vitro* antifungal data, as depicted in Table 3, indicated that some target coumarins displayed moderate inhibitory potencies against the tested fungal strains. It was obviously found that the antifungal efficiency of the synthesized compounds roughly complied with the rules in their antibacterial ability, though relatively weaker than the latter. Surprisedly, imidazoyl ethanol **13e** was sensitive to *C. albicans* and mono-methyl tetrazolyl ethanol modified coumarin **6b** exhibited excellent activity with MIC value of 4 μg/mL against *A. flavus* in comparison with Fluconazole (MIC=256 μg/mL).

Table 2 *In vitro* antibacterial data as MIC (μg/mL) for compounds **4**–**9** and **13**–**17** [a)]

Compounds	Gram-positive bacteria			Gram-negative bacteria		
	MRSA	*B. subtilis*	*M. luteus*	*E. coli*	*P. aeruginosa*	*S. dysenteriae*
4a	512	512	512	>512	512	512
4b	128	512	512	512	512	512
4c	>512	512	256	128	256	256
4d	32	32	32	64	64	64
4e	256	512	256	256	512	256
5	32	32	16	64	4	32
6a	256	512	256	512	512	128
6b	16	256	64	128	8	256
7a	16	16	32	16	32	64
7b	128	128	128	256	256	128
8	128	512	512	128	512	512
9	64	256	256	32	256	256
13a	512	512	128	256	256	512
13b	512	>512	128	>512	>512	>512
13c	512	>512	256	>512	256	512
13d	>512	512	128	512	256	256
13e	256	512	256	256	512	512
14	8	16	32	1	32	16
15a	>512	>512	256	512	512	>512
15b	512	512	32	512	256	512
16a	32	64	16	32	32	64
16b	512	>512	512	>512	>512	512
17	512	>512	>512	>512	>512	512
Chloramphenicol	16	32	8	32	32	16
Norfloxacin	8	4	2	1	16	16

a) MRSA, methicillin-resistant *Staphylococcus aureus N315*; *B. Subtilis*, *Bacillus subtilies* ATCC 21216; *M. luteus*, *Micrococcus luteus* ATCC 4698; *E. Coli*, *Escherichia coli* JM 109; *P. aeruginosa*, *Pseudomonas aeruginosa* ATCC 27853; *S. dysenteriae*, *Shigella dysenteriae*.

Table 3 *In vitro* antifungal data as MIC (μg/mL) for compounds **4**–**9** and **13**–**17** [a)]

Compounds	Fungi				
	CU	AF	BY	CA	CM
4a	512	512	>512	128	512
4b	256	256	512	512	128
4c	512	256	256	256	128
4d	256	64	128	4	32
4e	512	256	256	128	256
5	4	16	32	4	16
6a	512	128	256	64	512
6b	64	4	64	32	32
7a	16	256	8	4	16
7b	128	64	512	256	256
8	512	512	512	512	512
9	64	32	256	128	256
13a	512	512	128	64	512
13b	>512	512	>512	16	256
13c	256	256	512	512	128
13d	512	128	256	128	256
13e	256	256	512	2	128
14	4	32	32	1	4
15a	>512	>512	512	256	512
15b	512	512	>512	16	256
16a	16	256	32	8	16
16b	>512	512	>512	>512	512
17	256	512	512	512	128
Fluconazole	8	256	16	1	4

a) CU, *Candida utilis*; AF, *Aspergillus flavus*; BY, *Beer yeast*; CA, *Candida albicans* ATCC 76615; CM, *Candida mycoderm*.

While bis-triazolyl ethanol coumarin **14** showed the strongest inhibition towards *C. albicans* and *C. mycoderma*, which was equivalent to the reference drug Fluconazole with MIC values of 1 and 4 μg/mL, respectively. This demonstrated that triazolyl ethanol fragment was important for the exhibition of antifungal efficiency for the prepared coumarins.

3.3.3 Analysis of logP_{ow} values

logP_{ow} value governs various biological processes such as the transportation, distribution, metabolism and secretion of biological molecules. A good knowledge of logP_{ow} value is essential to predict the transportation and activity of drugs.

Usually, the data of logP_{ow} is analyzed according to the following equation:

$$\log P_{ow} = \log\left(\frac{C_o}{C_w}\right) \quad (1)$$

where C_o is the concentration of compound in the octanol phase and C_w is the concentration in the aqueous phase when the system is at equilibrium.

The obtained results given in Table 4 indicated that compounds **5**, **6b**, **7a**, **9**, **14** and **16a** with relatively low logP_{ow} values showed good antibacterial and antifungal activities in comparison with other target compounds with high logP_{ow} values. These might be responsible for the possibility that higher lipophilic compounds were difficult to be delivered to the binding sites in organism. Therefore, suitable lipophilicity is quite essential in drug design.

3.4 Preliminary action mechanism study

DNA is the informational molecule of almost all known living organisms. In medicinal chemistry, DNA is often viewed as the main cellular target for small molecules of biological importance such as carcinogens, steroids, and several classes of drugs. In recent years, with the increasing focus on the rational design and construction of new and more efficient drugs targeted to DNA, more and more interest in exploring the binding of small molecules with DNA is growing. Generally, electrostatic interaction (electrostatic attractions with the anionic sugar-phosphate backbone of DNA), groove binding (interactions with the DNA groove) and intercalation between the base pairs are the three noncovalent modes for small molecules binding with double-helix DNA [26]. To explore the possible antimicrobial action mechanism of title compounds, in this paper, the most active compound **14** was selected as representative one, and calf thymus DNA was selected as DNA model due to its medical importance, low cost and ready availability properties.

3.4.1 Absorption spectra of DNA in the presence of compound **14**

Absorption spectroscopy is one of the most useful techniques

Table 4 logP_{ow} values of compounds **4**–**9** and **13**–**17** [a)]

Compounds	logP_{ow}	Compounds	logP_{ow}	Compounds	logP_{ow}
4a	1.66±0.02	**7a**	0.60±0.03	**13e**	2.26±0.04
4b	1.89±0.03	**7b**	2.03±0.03	**14**	0.65±0.03
4c	NE	**8**	2.08±0.02	**15a**	–0.35±0.02
4d	NE	**9**	0.69±0.02	**15b**	1.99±0.02
4e	2.15±0.01	**13a**	–0.57±0.02	**16a**	0.48±0.02
5	0.45±0.02	**13b**	2.45±0.01	**16b**	2.07±0.01
6a	1.83±0.02	**13c**	NE	**17**	1.59±0.03
6b	0.55±0.04	**13d**	NE		

a) NE means no experimental data. It is difficult to obtain the logP_{ow} data of compounds **4c**–**4d** and **13c**–**13d** due to their quite low water solubility.

in DNA-binding studies. When compound binds to DNA, the absorbance spectrum will show hypochromism and hyperchromism because of the stacking interaction between an aromatic chromophore and the base pairs of DNA. Hyperchromism and hypochromism were regarded as spectral features for DNA double-helix structural change when DNA reacted with other molecules. With a fixed concentration of DNA, UV-Vis absorption spectra were recorded with the increasing amount of compound **14**. As shown in Figure 3, the absorption peak of DNA at 260 nm exhibited gradual increase and slight blue shift with the increasing concentration of compound **14**. The inset in Figure 3 showed that the measured absorption values of DNA-**14** complex were weaker than the simply sum of free DNA and free compound **14**, which meant a weak hypochromic effect existed between DNA and compound **14**. This hypochromic effect and the slight blue spectral shift suggested that coumarin **14** could actually interact with DNA, thus the binding mode of compound **14** with DNA was deserved to be further investigated.

On the basis of variations in the absorption spectra of DNA upon binding to **14**, Eq. (2) [27] can be utilized to calculate the binding constant (K).

$$\frac{A^0}{A-A^0}=\frac{\xi_C}{\xi_{D\text{-}C}-\xi_C}+\frac{\xi_C}{\xi_{D\text{-}C}-\xi_C}\times\frac{1}{K[Q]} \quad (2)$$

where A^0 and A represent the absorbance of DNA in the absence and presence of compound **14** at 260 nm, ξ_C and $\xi_{D\text{-}C}$ are the absorption coefficients of compound **14** and **14**-DNA complex, respectively. The plot of $A^0/(A-A^0)$ versus 1/[compound **14**] is constructed by using the absorption titration data and linear fitting (Figure 4), yielding the binding constant, K=4.20×10^3 L/mol, R=0.9977 (R is the correlation coefficient).

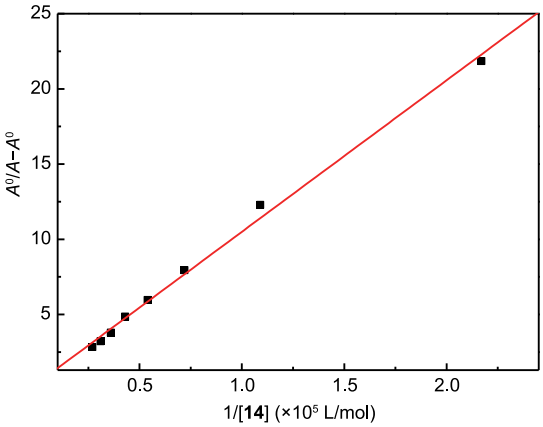

Figure 4 The plot of $A^0/(A-A^0)$ versus 1/[compound **14**].

3.4.2 Absorption spectra of competitive interaction of compound **14** and NR with DNA

Neutral Red (NR) is a planar phenazine dye structurally similar to acridine, thiazine, and xanthene kind. Compared with other common dyes, NR is lower toxicity, higher stability and convenient application, and in recent years, it has been demonstrated that the binding of NR with DNA is an intercalation binding. Thus it is always employed as a spectral probe to investigate the binding mode of small molecule with DNA. Therefore, the absorption spectra of NR and compound **14** interacted with DNA were investigated to further understand the binding mode between compound **14** and DNA in the present work.

The absorption peak of NR at around 460 nm showed gradual decrease with the increasing concentration of DNA, and a new band at around 530 nm developed (Supporting Information online). This was attributed to the formation of the new DNA-NR complex. Figure 5 displayed the absorption spectra

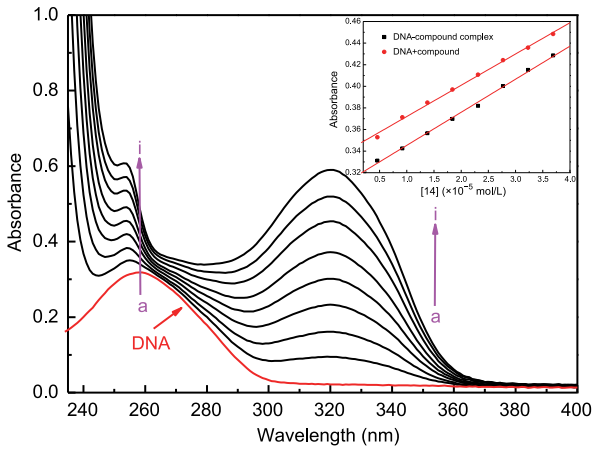

Figure 3 Absorption spectra of DNA with different concentrations of compound **14** (pH 7.4, T=290 K). Inset: comparison of absorption at 260 nm between the **14**-DNA complex and the sum values of free DNA and free compound **14**. c(DNA)=5.28×10^{-5} mol/L, and c(compound **14**)=0–3.69×10^{-5} mol/L for curves (a–i) respectively at increment 0.46×10^{-5} (color online).

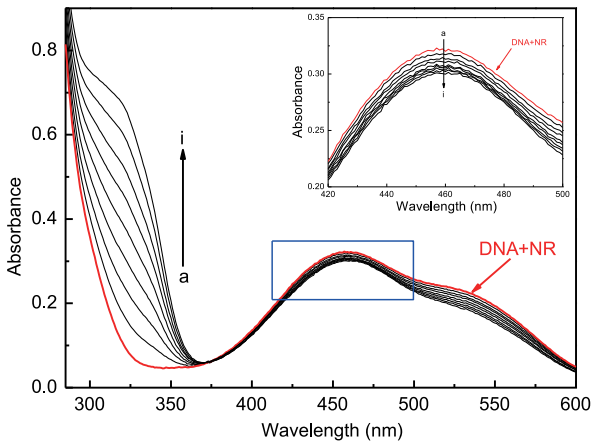

Figure 5 Absorption spectra of the competitive reaction between **14** and NR with DNA. c(DNA)=5.28×10^{-5} mol/L, c(NR)=2×10^{-5} mol/L, and c(compound **14**)=0–3.69×10^{-5} mol/L for curves (a–i) respectively at increment 0.46×10^{-5}. Inset: absorption spectra of the system with the increasing concentration of **14** in the wavelength range of 420–500 nm (color online).

of a competitive binding between **14** and NR with DNA. As shown, with the increasing concentration of compound **14**, both the maximum absorption around 460 and 530 nm decreased. Compared with the absorption band at around 460 nm of the free NR in the presence of the increasing concentrations of DNA, the spectra in Figure 5 exhibited that compound **14** interacted with DNA not by substituting for NR in the DNA-NR complex. The results suggested that the binding mode of compound **14** with DNA might be not intercalation binding.

3.4.3 Measurement of fluorescence spectra

The fluorescence quenching spectra of compound **14** with growing amounts of DNA at the excitation wavelength of 323 nm are shown in Figure 6. The fluorescence intensity of compound **14** at around 431 nm regularly decreased, but the maximum emission wavelength of compound **14** did not apparently shift with the increase of DNA concentration. The results indicated that DNA could quench the intrinsic fluorescence of compound **14** and the binding of compound **14** with DNA indeed exists.

Dynamic quenching and static quenching are the two well-known quenching processes. Dynamic quenching is a process that the fluorophore and the quencher come into contact during the transient existence of the excited state, while static quenching is the formation of fluorophore and quencher complex. The method to distinguish static and dynamic quenching is to calculate their different binding constants dependent on temperature or viscosity or to measure their lifetimes. In this work, the calculation of binding constant dependent on the temperature was employed to elucidate the quenching mechanism.

The fluorescence quenching data can be analyzed by the well-known Stern-Volmer equation [28]:

$$\frac{F_0}{F}=1+K_{SV}[Q] \tag{3}$$

where F_0 and F represent fluorescence intensity of compound **14** in the absence and presence of DNA, respectively. K_{SV} (L/mol) is the Stern-Volmer quenching constant, and [Q] is the concentration of DNA. The Stern-Volmer equation was applied to determine K_{SV} by linear regression of a plot of F_0/F against [Q]. Hence, the value of K_{SV} at different temperatures could be calculated and was shown in Figure 7.

It is demonstrated that in dynamic quenching, the quenching constants are expected to increase with a gradually increasing temperature due to larger diffusion coefficients. While the increase of temperature is likely to result in a smaller K_{SV} in static quenching due to the dissociation of weakly bound complexes. Figure 7 showed that the Stern-Volmer quenching constant, K_{SV}, decreased linearly with increasing temperatures. These calculated K_{SV} were 2.24×10^4 (R=0.9999), 1.52×10^4 (R=0.9999) and 0.89×10^4 (R=0.9999)

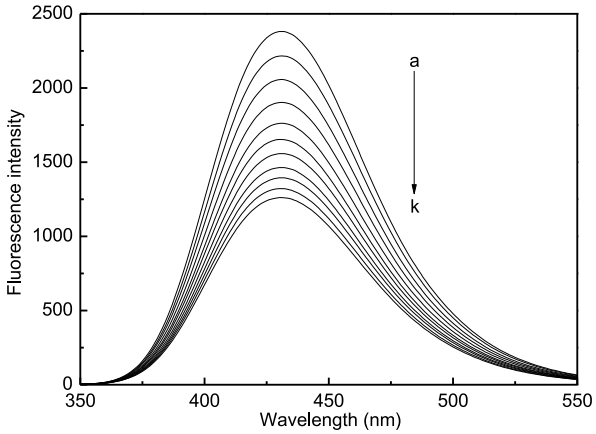

Figure 6 Fluorescence spectra of compound **14** in the presence of DNA at different concentrations (pH 7.4, T=290 K, λ_{ex}=323 nm, λ_{em}=431 nm). c(compound **14**)=4.61×10^{-5} mol/L, and c(DNA)=0, 0.40×10^{-5}, 0.79×10^{-5}, 1.19×10^{-5}, 1.58×10^{-5}, 1.98×10^{-5}, 2.38×10^{-5}, 2.77×10^{-5}, 3.17×10^{-5}, 3.56×10^{-5} and 3.96×10^{-5} mol/L for curves (a–k), respectively.

L/mol at 290, 300 and 310 K, respectively, at pH 7.4. Thus, the fluorescence quenching mechanism of compound **14** interacted with DNA was revealed to be the consequence of static quenching.

Therefore, the fluorescence quenching of compound **14** by DNA could be described by the modified Stern-Volmer equation [29]:

$$\frac{F_0}{\Delta F}=\frac{1}{f_a K_a}\frac{1}{[Q]}+\frac{1}{f_a} \tag{4}$$

where ΔF is the difference in fluorescence intensity of compound **14** in the absence and presence of DNA at concentration [Q], f_a is the fraction of accessible fluorescence, and K_a is the effective quenching constant for the accessible fluorophores, which are analogous to associative binding constants for the quencher-acceptor system. The dependence of $F_0/\Delta F$ on the reciprocal value of quencher concentration

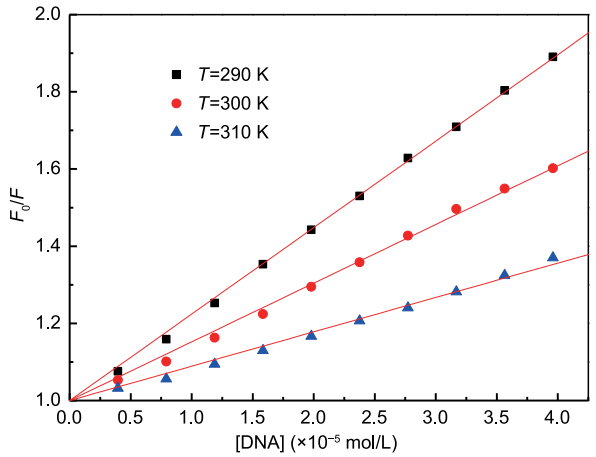

Figure 7 Stern-Volmer plots for the fluorescence quenching of compound **14** by DNA at different temperatures.

1/[Q] is linear with the slope equaling to the value of $1/(f_aK_a)$. The value of $1/f_a$ is fixed on the ordinate. The constant K_a is a quotient of the ordinate $1/f_a$ and the slope $1/(f_aK_a)$. The modified Stern-Volmer plots were showed in Figure 8 and the calculated results were depicted in Table 5. The decreasing trend of K_a with increasing temperature was in accordance with K_{SV}'s as discussed above, which accorded with static quenching.

3.4.4 Thermodynamic analysis and the nature of the binding forces

Generally, hydrogen bonds, van der Waals force, hydrophobic force, and electrostatic interactions are the main noncovalent interaction force between small molecules and biomolecules. The main evidence to confirm the binding force is the thermodynamic parameters of binding reaction. If the enthalpy change (ΔH) does not vary significantly over the studied temperatures range, then its value and that of entropy change (ΔS) can be determined from the van't Hoff equation [30]:

$$\ln K = -\frac{\Delta H}{RT} + \frac{\Delta S}{R} \quad (5)$$

where K is analogous to the associative binding constants at the corresponding temperature and R is the gas constant. The temperatures used were 290, 300 and 310 K, respectively. The values of ΔH and ΔS were obtained from the slope and intercept of the linear van't Hoff plot based on $\ln K_a$ versus $1/T$ (Figure 9). The free energy change (ΔG) was then calculated from the following equation [31]:

$$\Delta G = \Delta H - T\Delta S \quad (6)$$

Table 6 listed the thermodynamic parameters for the interaction of compound **14** with DNA. The negative values of ΔG suggested that the binding process was spontaneous. The negative values of ΔH indicated that the binding process was mainly enthalpy driven and by means of hydrogen binding interactions [32]. The negative ΔS value is frequently taken as an evidence for van der Waals force. Therefore, $\Delta H<0$ and $\Delta S<0$ obtained in this case indicated that both hydrogen bonds and van der Waals force played an important role in the binding of compound **14** to DNA and contribute to the stability of the complex.

3.4.5 Iodide quenching studies

It is well known that the highly negatively charged quencher is expected to be repelled by the negatively charged phosphate backbone of DNA. Therefore, if a molecule is protected from being quenched by anionic quencher, the binding mode of the small molecule with DNA is intercalation. While different from intercalation, groove binding provides much less protection for the bound molecule [33]. The value of quenching constants (K_{SV}) of the groove binding should be higher than that of the molecule bound to DNA by intercalative bound. Negatively charged I^- ion was selected for this purpose. The values of K_{SV} of compound **14** by I^- ion in the absence and presence of DNA were calculated to be 72.82 (R=0.9982) and 79.49 (R=0.9985) L/mol, respectively, by the Stern-Volmer equation (Figure 10). The results showed that iodide quenching effect was increased when compound **14**

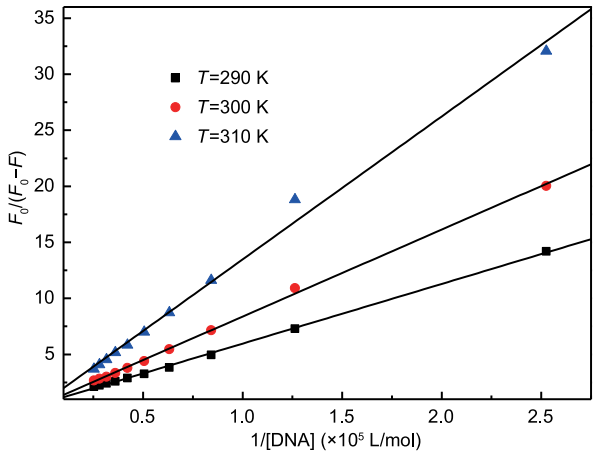

Figure 8 Modified Stern-Volmer plots for the fluorescence quenching of compound **14** by DNA at different temperatures.

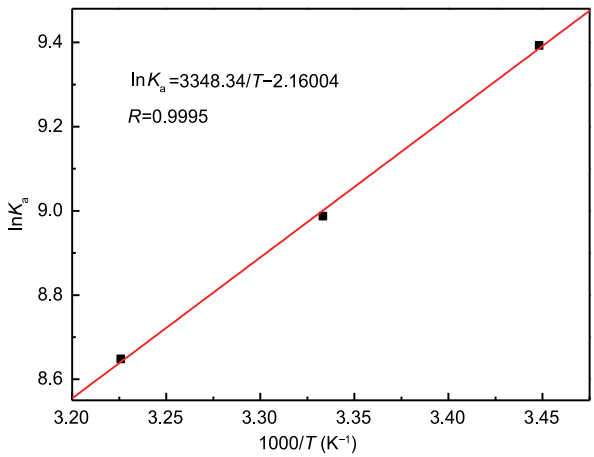

Figure 9 van't Hoff plots of the **14**-DNA system.

Table 5 Modified Stern-Volmer quenching constants for the interaction of compound **14** with DNA at various temperatures

pH	T (K)	K_a (L/mol)	R
7.4	290	1.20×10^4	0.9995
	300	0.80×10^4	0.9994
	310	0.57×10^4	0.9965

Table 6 Thermodynamic parameters of **14**-DNA system at different temperatures

T (K)	ΔH (kJ/mol)	ΔG (kJ/mol)	ΔS (J/(mol K))
290		−22.63	
300	−27.84	−22.45	−17.96
310		−22.27	

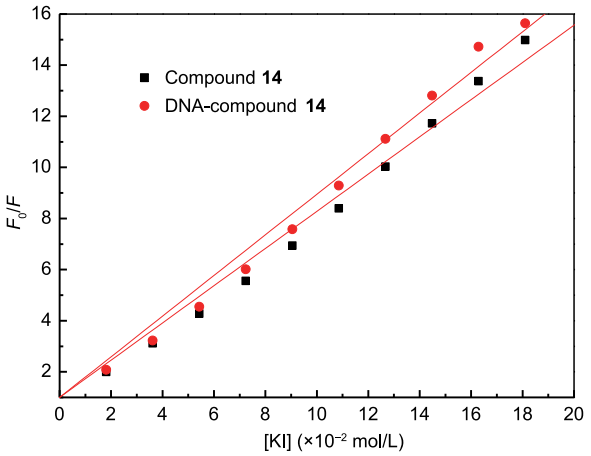

Figure 10 Fluorescence quenching plots of compound **14** by KI in the absence and presence of DNA at pH 7.4 and 290 K. c(compound **14**)=4.61×10^{-5} mol/L, and c(DNA)=2.64×10^{-5} mol/L.

was bound to DNA, suggesting that the binding mode of compound **14** with DNA might be of groove binding nature.

4 Conclusions

In conclusion, a series of coumarin-derived azolyl ethanols were synthesized through convenient and economic synthetic procedures. All the target compounds were characterized by IR, ^{1}H NMR, ^{13}C NMR, and HRMS spectra. Their *in vitro* antibacterial and antifungal activities indicated that some of the synthesized coumarin-derived azolyl ethanols with suitable logP_{ow} values could effectively inhibit the growth of all the tested strains, and even displayed equipotent or superior activities to the current clinical drugs. Notably, compound **14** gave remarkable antibacterial and antifungal activities in comparison with the reference drugs Chloramphenicol, Norfloxacin and Fluconazole. The interaction of compound **14** with calf thymus DNA displayed that compound **14** could interact with DNA through groove binding driven by hydrogen bonds and van der Waals force to form **14**-DNA complex to exert its powerful antibacterial and antifungal activities.

Acknowledgments This work was supported by the National Natural Science Foundation of China (21172181, 21372186, 81450110094, 81250110089, 81350110338), the Key Program from Natural Science Foundation of Chongqing (CSTC2012jjB10026) and the Specialized Research Fund for the Doctoral Program of Higher Education of China (SRFDP 20110182110007).

Conflict of interest The authors declare that they have no conflict of interest.

Supporting information The supporting information is available online at http://chem.scichina.com and http://link.springer.com/journal/11426. The supporting materials are published as submitted, without typesetting or editing. The responsibility for scientific accuracy and content remains entirely with the authors.

1 a) Ferreira BS, de Almeida AM, Nascimento TC, de Castro PP, Silva VL, Diniz CG, Hyaric ML. *Bioorg Med Chem Lett*, 2014, 24: 4626–4629; b) Lv JS, Peng XM, Kishore B, Zhou CH. *Bioorg Med Chem Lett*, 2014, 24: 308–313
2 Hopkins AL, Bickerton GR, Carruthers IM, Boyer SK, Rubin H, Overington JP. *Curr Top Med Chem*, 2011, 11: 1292–1300
3 a) Peng XM, Cai GX, Zhou CH. *Curr Top Med Chem*, 2013, 13: 1963–2010; b) Zhang YY, Zhou CH. *Bioorg Med Chem Lett*, 2011, 21: 4349–4352
4 a) Alwan WS, Karpoormath R, Palkar MB, Patel HM, Rane RA, Shaikh MS, Kajee A, Mlisana KP. *Eur J Med Chem*, 2015, 95: 514–525; b) Brown GD, Denning DW, Levitz SM. *Science*, 2012, 336: 647; c) Wei JJ, Jin L, Wan K, Zhou CH. *Bull Korean Chem Soc*, 2011, 32: 229–238; d) Benincasa M, Pacor S, Wu W, Prato M, Bianco A, Gennaro R. *ACS Nano*, 2011, 5: 199–208; e) Zou Y, Yu SC, Li RW, Zhao QJ, Li X, Wu MC, Huang T, Chai XX, Hu HG, Wu QY. *Eur J Med Chem*, 2014, 74: 366–374
5 Dione N, Khelaifia S, Lagier JC, Raoult D. *Int J Antimicrob Agents*, 2015, 45: 537–540
6 Zhang L, Peng XM, Damu GLV, Geng RX, Zhou CH. *Med Res Rev*, 2014, 34: 340−437
7 a) Fang B, Zhou CH, Rao XC. *Eur J Med Chem*, 2010, 45: 4388–4398; b) Li LJ, Ding H, Wang BG, Yu SC, Zou Y, Chai XY, Wu QY. *Bioorg Med Chem Lett*, 2014, 24: 192–194
8 Babazadeh-Qazijahani M, Badali H, Irannejad H, Afsarian MH, Emami S. *Eur J Med Chem*, 2014, 76: 264–273
9 Wang Y, Damu GLV, Lv JS, Geng RX, Yang DC, Zhou CH. *Bioorg Med Chem Lett*, 2012, 22: 5363–5366
10 Zhang L, Kannekanti VK, Syed R, Geng RX, Zhou CH. *Chem Biol Drug Des*, 2015, 96: 648–655
11 Cui SF, Ren Y, Zhang SL, Peng XM, Damu GLV, Geng RX, Zhou CH. *Bioorg Med Chem Lett*, 2013, 23: 3267–3272
12 Kumar GVS, Rajendraprasad Y, Mallikarjuna BP, Chandrashekar SM, Kistayya C. *Eur J Med Chem*, 2010, 45: 2063–2074
13 Bonanomi G, Braggio S, Capelli AM, Checchia A, Fabio RD, Marchioro C, Tarsi L, Tedesco G, Terreni S, Worby A, Heibreder C, Micheli F. *ChemMedChem*, 2010, 5: 705–715
14 a) Bhatia MS, Zarekar BE, Choudhari PB, Ingale KB, Bhatia NM. *Med Chem Res*, 2011, 20: 116–120; b) Kalhor M, Mobinikhaledi A, Dadras A, Tohidpour M. *J Heterocycl Chem*, 2011, 48: 1366–1370; c) Tamilselvi A, Mugesh G. *Bioorg Med Chem Lett*, 2010, 20: 3692–3697; d) Wang QP, Zhang JQ, Damu GLV, Wan K, Zhang HZ, Zhou CH. *Sci China Chem*, 2012, 55: 2134–2153
15 a) Parvez A, Meshram J, Tiwari V, Sheik J, Dongre R, Youssoufi MH, Ben Hadda T. *Eur J Med Chem*, 2010, 45: 4370–4378; b) Arshad A, Osman H, Bagley MC, Lam CK, Mohamad S, Zahariluddin ASM. *Eur J Med Chem*, 2011, 46: 3788–3794; c) Patel D, Patel R, Kumari P, Patel N. *Med Chem Res*, 2012, 21: 1611–1624; d) Damu GLV, Cui SF, Peng XM, Wen QM, Cai GX, Zhou CH. *Bioorg Med Chem Lett*, 2014, 24: 3605–3608
16 Peng XM, Damu GLV, Zhou CH. *Curr Pharm Des*, 2013, 19: 3884–3930
17 Shi Y, Zhou CH. *Bioorg Med Chem Lett*, 2011, 21: 956–960
18 Shi Y, Zhou CH, Zhou XD, Geng RX, Ji QG. *Acta Pharm Sinica*, 2011, 46: 798–810
19 a) Zhang SL, Damu GLV, Zhang L, Geng RX, Zhou CH. *Eur J Med Chem*, 2012, 55: 164–175; b) Wang XL, Wan K, Zhou CH. *Eur J Med Chem*, 2010, 45: 4631–4639; c) Damu GLV, Wang QP, Zhang HZ, Zhang YY, Lv JS, Zhou CH. *Sci China Chem*, 2013, 56: 952–969; d) Zhang HZ, Damu GLV, Cai GX, Zhou CH. *Eur J Med Chem*, 2013, 64: 329–344; e) Zhang HZ, Wei JJ, Kannekanti VK, Rasheed S, Zhou

CH. *Med Chem Res*, 2015, 24: 182–196
20 Cui SF, Peng LP, Zhang HZ, Rasheed S, Kannekanti VK, Zhou CH. *Eur J Med Chem*, 2014, 86: 318–334
21 Zhou CH, Wang Y. *Curr Med Chem,*, 2012, 19: 239–280
22 Fosso MY, Zhu HK, Green KD, Garneau-Tsodikova S, Fredrick K. *ChemBioChem*, 2015, doi: 10.1002/cbic.201500256
23 a) Li XL, Hu YJ. *Biomacromolecules*, 2012, 13: 873–880; b) Luo YL, Baathulaa K, Kannekanti VK, Zhou CH, Cai GX. *Sci China Chem*, 2015, 58: 483–494; c) Peng LP, Nagarajan S, Rasheed S, Zhou CH. *Med Chem Commun*, 2015, 6: 222–229; d) Yin BT, Yan CY, Peng XM, Zhang SL, Rasheed S, Geng RX, Zhou CH. *Eur J Med Chem*, 2014, 71: 148–159; e) Hu YJ, Liu Y, Xiao XH. *Biomacromolecules*, 2009, 10: 517–521
24 Sinhamahapatra A, Sutradhar A, Pahari A, Bajaj HC, Panda AB. *Appl Catal A*, 2011, 394: 93–100
25 National Committee for Clinical Laboratory Standards Approved standard Document. M27-A2, Reference Method for Broth Dilution Antifungal Susceptibility Testing of Yeasts, National Committee for Clinical Laboratory Standards, Wayne, PA, 2002
26 Zhang GW, Fu P, Wang L, Hu MM. *J Agric Food Chem*, 2011, 59: 8944–8952
27 a) Devi CV, Singh NR. *Spectrochim Acta A*, 2011, 78: 1180–1186; b) Dai LL, Zhang HZ, Nagarajan S, Rasheed S, Zhou CH. *Med Chem Commun*, 2015, 6: 147–154; c) Zhang HZ, Lin JM, Rasheed S, Zhou CH. *Sci China Chem*, 2014, 57: 807–822
28 Lakowicz JR. *Principles of Fluorescence Spectroscopy.* 3rd Ed. New York: Springer, 2006. 11–12
29 Yang MM, Xi XL, Yang P. *Chin J Chem*, 2006, 24: 642–648
30 Zhao N, Wang XM, Pan HZ, Hu YM, Ding LS. *Spectrochim Acta A*, 2010, 75: 1435–1442
31 Ortiz M, Fragoso A, Ortiz PJ, O'Sullivan CK. *J Photochem Photobiol A*, 2011, 218: 26–32
32 Yuan JL, Liu H, Kang X, Lv Z, Zou GL. *J Mol Struct*, 2008, 891: 333–339
33 Akbay N, Seferoğlu Z, Gök E. *J Fluoresc*, 2009, 19: 1045–1051